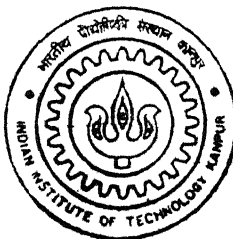


STUDIES ON DIFFUSED INDOOR OPTICAL WIRELESS SYSTEMS

by

N. Janardhan

TH
EE/2001/M
J251s



DEPARTMENT OF ELECTRICAL ENGINEERING
INDIAN INSTITUTE OF TECHNOLOGY, KANPUR

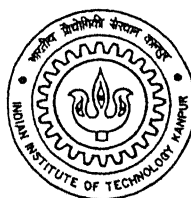
February, 2001

STUDIES ON DIFFUSED INDOOR OPTICAL WIRELESS SYSTEMS

A Thesis Submitted
in Partial Fulfillment of the Requirements
for the degree of
Master of Technology

by

N.Janardhan



to the

**DEPARTMENT OF ELECTRICAL ENGINEERING
INDIAN INSTITUTE OF TECHNOLOGY
KANPUR**

February, 2001

A133748

Dedicated

To

Dr. Joseph John and his family

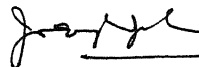
(my thesis supervisor and his family members)

For their unconditional love and support.

CERTIFICATE

20-201
M. J. P.

This is to certify that the thesis work entitled "**STUDIES ON DIFFUSED INDOOR OPTICAL WIRELESS SYSTEMS**" by *N. Janardhan*, Roll no. 9910453 has been carried under my supervision and the same has not been submitted elsewhere for a degree.



Dr. Joseph John
Associate Professor
Department of Electrical Engineering
I.I.T. Kanpur -208016

Feb, 2001

ACKNOWLEDGEMENTS

I am most indebted and grateful to my guide **Dr. Joseph John** for his encouragement and valuable guidance throughout my work. He is always very patient and cooperative to me while discussing the various aspects of the work. He is always available to me whenever I need inspite of his busy schedule. Without him it would have been impossible to conceive this.

I would like to thank his family, who always encouraged me morally. Their helping nature is unlimited.

I would like to thank Chaturi Singh for his helping nature and moral support in experimental work.

I am very grateful to my great friend N.V.Ramana , who is always very gentle , patient and kind hearted, helping and suggest me always. My sincere thanks to Swarna Bhai who helped me in experimental work. I am grateful to Sanjay and Alok who helped and cooperated in the lab. I am grateful to my friends Venu, Srilakshmi, Vibha, Naidu, Chakrapani, Sasi, Samba, Sunder raju, Ravindhra, Krishna rao, Bhanu, Sekhar, Praveen, D.K.Singh, Viswanath, Godwin, Kushwaah, Sushil, Sriram, Prabhakar, Murali. My sincere thanks to Doordarshan department who gave me nice opportunity to do M.Tech programme in IIT Kanpur.

I wish to acknowledge the constant encouragement, support and blessings which my family gave me.

N.Janardhan.

CONTENTS

	Page No.
CHAPTER 1 : INTRODUCTION	
1.1 Introduction.....	1
1.2 Indoor Optical Wireless Systems.....	2
1.2.1. Point – to – Point links.....	2
1.2.2. Optical Tele-point system.....	3
1.3 Present work.....	3
1.4 Thesis layout.....	4
CHAPTER 2 : REVIEW OF DIFFUSED INFRARED SYSTEMS	
2.1 Introduction.....	5
2.2 The IRDA Standard for very short distance Point-to-point.....	7
2.3 Other Standards used in Diffused Infrared systems.....	8
2.3.1 Different IEEE 802 standards.....	8
2.3.2 Scope of effort of IEEE 802.11 standard.....	9
2.4 Comparison between Radio and Optical Diffused Wireless systems...	10
CHAPTER 3: DESIGN OF A DIFFUSED INDOOR INFRARED LINK	
3.1 Choice of System Elements	12
3.1.1 Choice of Source	12
3.1.2 Choice of Detector	13
3.1.3 Choice of Receiver Front –end	15
3.2 Limitations of the System Elements	16

3.3	Measures of System Performance	16
3.4	Theoretical Models for Prediction of Optical Power at a Point	17
3.4.1	Power transfer Model from a Radiating Surface with Angular distribution(Model 1)	17
3.4.2	LED Source to Receiver power transfer assuming Uniform Power Distribution (Model-2).	20
3.4.3	LED source to Receiver Power Transfer assuming LED beam to be Gaussian (Model-3).	24
3.4.3.1	Properties of Fundamental Gaussian Beam.	27
3.4.3.2	Power received for Finite Longitudinal offsets.	27

CHAPTER 4: SYSTEM IMPLEMENTATION AND PERFORMANCE

4.1	LED Sources	29
4.1.1	Measurement of Source characteristics.	29
4.2	Pseudo Random Bit Sequence (PRBS) Generator	35
4.3	Transmitter Circuit (Driver Circuit)	36
4.4	Receiver Circuit	37
4.4.1	Detector and the Pre-amplifier circuit	37
4.4.2	Peak detector circuits	38
4.4.3	Summer using Op-amplifier	39
4.4.4	Comparator Circuit using NE529	39
4.5	Receiver Characterisation	40
4.5.1	Receiver Sensitivity	40
4.5.2	Dynamic range	40
4.5.3	Maximum Data Rate	40

4.6	System Measurements and Performance	40
4.6.1	Longitudinal separation Measurement	41
4.6.2	Lateral Separation Measurement	41
4.7	Comparison of Theoretical and Measured results.	41
CHAPTER 5. RESULTS, CONCLUSIONS AND SUGGESIONS FOR FUTURE WORK		50
REFERENCES51.

List of Figures

3.1 Arbitrary orientation of emitting and receiving surfaces.....	18
3.2 Arbitrarily oriented differential surface areas dA_S and dA_R	19
3.3 $B(\theta)$ patterns for different n values.....	21
3.4 Normalised variation of power as a function of distance.....	22
3.5 Uniform power model geometry.....	23
3.6 Coupling efficiency for different θ values of the cone.....	25
3.7 Gaussian Far Field Patterns.....	26
4.1 Current – Intensity characteristics – set up.....	30
4.2 Current – Intensity characteristic-results.....	30
4.3 Far field measurement set up.....	31
4.4 Far field pattern of Round type of IR LED.....	32
4.5 Far field pattern of Cut type of IR LED.....	32
4.6 Far field pattern of array(3no.s) of IR LED.....	33
4.7 Far field pattern of array(5no.s) of IR LED.....	33
4.8 Arrangement of LEDs in the array LED sources.....	34
4.9 PRBS generator circuit.....	35
4.10a. LED driver circuit with single LED.....	36
4.10b. LED driver circuit with cascade of two LEDs.....	37
4.11. Receiver circuit.....	37
4.12 Longitudinal separation of Round type of IR LED.....	42
4.13 Longitudinal separation of Cut type of IR LED.....	42
4.14 Longitudinal separation of array(3no.s) of IR LED.....	43
4.15 Longitudinal separation of array(5no.s) of IR LED.....	43
4.16 Lateral separation of Round type of IR LED.....	44
4.17 Lateral separation of Cut type of IR LED.....	44
4.18 Lateral separation of array(3no.s) of IR LED.....	45

4.19 Lateral separation of array(5no.s) of IR LED.....	45
4.20 Comparison of expt. Values with long. Uniform of Round type IR LED.....	46
4.21 Comparison of expt. Values with long. Uniform of Cut type IR LED.....	46
4.22 Comparison of expt. Values with long. Uniform of array(3nos) of IR LED.....	47
4.23 Comparison of expt. Values with long. Uniform of array(5nos) of IR LED.....	47
4.24 Longitudinal offset of Round type of IR LED	48
4.25 Longitudinal offset of Cut type of IR LED	48
4.26 Longitudinal offset of array(3nos) of IR LED	49
4.27 Longitudinal offset of array(5nos) of IR LED	49

ABSTRACT

Wireless Infrared (IR) communication systems are being used extensively because of their portability and low cost. In this thesis an attempt has been made to study Diffused Indoor Optical Wireless Systems. A diffused indoor link has been designed using LED as the source and PIN photodetector as the detector. Some simple theoretical models have been suggested to predict the optical power at a given point along the axis of the source. An experimental IR link was implemented using single LEDs and also using an array of LEDs. Sources were characterized and their far-field patterns were measured. These patterns were fitted to the suggested theoretical models.

Variation of optical power along the axis of the sources were measured and then compared with theory. The experimental indoor link had a data rate 200 kBits/sec and it achieved a range of 8cm using single LEDs and 20cm using multiple LEDs.

CHAPTER 1

INTRODUCTION

1.1 INTRODUCTION

With the spread of high performance portable computers and the need of network computers, data terminals and devices such as personal digital assistants (PDAs), wireless LANs have become an emerging technology for today's computers and communication industries. The advantages of wireless networks over wired network are their flexibility and lower cost. Due to physical limitations like ambient light interference, eye safety, transit time of LED and limited available bandwidth, optical wireless LANs are currently targeted to operate at data rates between 1-20 M b/s.

1.2 IN DOOR OPTICAL WIRELESS SYSTEMS

In the past few years, the growth of data communication has been enormous. Data communication has been established using wired physical connections. These physical connections introduce difficulties in construction and rewiring during the system set up and expansion phases. An alternative that achieves the same goal for data communication while offering mobility is the wireless network. Traditionally, radio frequency transmission was used in wireless applications. However, the RF spectrum is so congested that it is very difficult to accommodate new high bit rate applications. The optical system with low implementation complexity and no spectrum license requirements provide a possible solution.

The use of an optical wireless network for indoor applications offers numerous advantages over the equivalent RF wireless network. The optical infrared energy can typically be contained within the room or communication environment easily, thus virtually eliminating the problems of interference generated by neighboring users while offering a degree of security at the physical level. The same transmitter equipment and optical wavelength can be reused in other parts of the building, thus offering spatial diversity. Moreover, optical wireless systems offer immunity from signal fading. As

such, indoor infrared communication has recently received much attention, especially in view of the increased data and mobility requirements of users for both computing and communications.

Indoor IR systems comes in the category of short distance systems. Indoor systems have the major advantage that the distances involved are much less than out door systems. There are primarily two types of indoor optical wireless systems, viz. Point –to – Point links and Optical Tele-point Systems.

1.2.1 Point-to-Point links

Indoor Point-to-point systems do not differ from the outdoor variety in their operating principles, however , in practice their designs are invariably very different. First, they must be Class I eye safe, which generally means that the optical source is an LED. This in turn limits the capacity to typically a few mega bits per second. On the other hand, Indoor systems need none of the weather proofing that Outdoor systems require and only operate over short distances; and hence they can be produced very cost effectively. Here a capacity of 10 Mb/s can be conveyed over a span of around 20m, such systems could be used, for example, to extend a 10 Mb/s LAN port to a different part of an office where no convenient port exists, or to link two separate offices via a link corridor.

Outdoor short distance systems, used perhaps to deliver high capacity links between neighboring buildings, enjoy the luxury, as do long distance systems, of utilizing a high power Class 3B emitter since these systems will be located away from people. A good power budget can therefore be achieved even with relatively simple components. This, combined with the low atmospheric loss, means that a higher free space loss can be tolerated in return for the convenience of a larger beam diameter at the receiver. Setting up and aligning these systems is then significantly easier than their long distance cousins, and furthermore, automatic alignment and tracking is not required. Consequently, overall complexity and cost is significantly reduced. The 1Gbit/s result over 40m is particularly interesting as it shows the order of capacity that can be achieved with today's technology.

1.2.2 Optical Tele-point System

Indoor applications, being fundamentally confined to short distance spans, are uniquely appropriate to optical wireless systems that utilize wide diverging beams rather than the narrow beams of point-to-point systems. Such systems are sometimes referred to as optical tele-point systems and afford a number of attractive features. Each cell created by an optical tele-point base station can be shared by as many users as can be accommodated within the cell. The cell diameters are 10m down to 0.5m. Each cell delivers a capacity of 10 Mb/s shared between users via conventional LAN protocols. The larger cells might be deployed in open offices, libraries, waiting rooms and hospital wards.

Transmitter sources in Optical wireless system:

There are two types of transmitter sources used in optical wireless systems, viz. light emitting diodes (LEDs) and laser diodes (LDs).

The optical fiber systems industry has spawned semiconductor LASERS with broad bandwidths and high launch powers, features which are equally attractive to optical wireless systems, particularly for outdoor applications. However, for indoor applications LASERS pose a potential safety hazard because they are a point source emitter. LEDs, on the other hand, are large area emitters, and thus can be operated safely, even at relatively high powers. They are therefore the preferred emitter for most indoor applications. To compensate for the lower powers that LEDs generally emit, arrays of them can be used as the optical source. The penalty, however is bandwidth. Whereas LASER speeds extend into the Gb/s regime, LEDs are typically limited to 10 Mb/s, perhaps extending to 50 Mb/s for some specialist devices.

1.3 PRESENT WORK

The major aim of the present work has been to study diffused indoor IR links both theoretically and experimentally. As part of the present work a simple IR indoor link has been designed using LED sources and PIN photodiodes. Some simple theoretical models are suggested for prediction of optical power along the axis of the optical sources. An

experimental IR link was implemented and tested and its performance measured. The measurements were compared with theoretical work.

1.4 THESIS LAYOUT

Chapter 2 of the thesis gives a detailed review of the different types of indoor IR systems. IRDA standards as well as IEEE standards for radio and optical wireless systems are also reviewed. Chapter 3 gives the different design aspects of an indoor IR system. System considerations for the choice of source, detector and receiver front-ends are discussed. Some theoretical models are suggested to study the variation of optical power along the axis of the sources. Theoretical results are also plotted. Details of the experimental IR system implemented are discussed in Chapter 4. It also gives details of source characterization. The measured power levels along the axis of different sources are also given and then compared with theory. The major results of the study are discussed in Chapter 5 and some suggestions for future work in this area are also given.

A detailed list of references used in this thesis work is given at the end.

CHAPTER 2

REVIEW OF DIFFUSED INFRARED SYSTEMS

A review of diffused infrared (IR) systems is given in this chapter. IrDA standards as well as IEEE standards for IR systems are also discussed.

2.1 INTRODUCTION

There are three different types of free space optical links, designated by their transmitter/ receiver types.

1. Point-to-Point or LOS system
2. Quasi- diffused systems
3. Diffused systems.

Point-to-Point or LOS System

The point-to-point systems are implemented by using IrDA Standards in Indoor Optical Wireless systems. In this section, the more objective study is on diffused system, because it has lot of advantages. The primary advantage of using the diffusive approach is that there is no need for accurate alignment between transmitter and receiver. This is especially important in portable applications, in which readjusting a receiver antenna after every movement is not practical. The main drawback of the diffusive approach is the temporal dispersion caused by reflections from ceilings and walls, which effectively limits the rate of transmission.

Quasi-diffused System

Quasi-diffused means diffusive and directed, i.e the reflections from the ceiling are diffuse and the transmitters & receivers are directed towards ceiling. The quasi-diffuse transmitter can be employed in conjunction with either a single-element or imaging

receiver. Such transmitters emit a collection of relatively narrow beams that illuminate a regular lattice of spots on the ceiling, the path loss can be reduced by quasi-diffuse or multi beam transmitter.

The imaging receiver, when used with maximal ratio combining (MRC), can be considered a “spatial matched filter ” when the quasi-diffuse transmitter is used with an imaging receiver, a synergistic performance enhancement occurs. The desired signal is concentrated in a small region, and the spatial matched filter is able to concentrate its observation on that region, rejecting as much ambient light noise as possible.

Quasi-diffuse transmitters are not much more complex to implement than single – beam transmitters, and provide more improvement in conjunction with imaging receivers. This is due to the fact that when used with imaging receivers, quasi –diffuse transmitters concentrate the signal in a small spot, thus allowing greater noise rejection.

$$\text{Path loss} = \text{transmitted power} / \text{received power} \quad (\text{path loss} > 1)$$

Although the quasi-diffuse transmitters uses narrow beams, eye safety can always be ensured by making the beam diameter sufficiently large. Furthermore, the power required in each beam is relatively low (of the order of a few mw) and modest beam divergence is acceptable.

Diffused Infrared System

The diffused system is converse to line-of-sight path system, which is employed in indoor systems. In this group of systems the beams, as well as radiating over a wide angle, are also allowed to reflect off surfaces and objects in the vicinity such as walls, ceiling, floor, and furniture. In addition, the field of view of the view of the optical receivers in the base and user stations is widened to such an extent that the line of sight as well as reflected light can be detected with the same ease. Such an arrangement goes some way toward guaranteeing that a signal path is always present, regardless of obstacles or people impeding the line-of-sight path. This arrangement also allows roaming to some degree. However, the penalty of diffuse transmission is a much reduced capacity compared with LOS systems. This is entirely a consequence of the multiple

signal paths reaching the receiver, which cause classic pulse spreading and inter symbol interference.

The upper bound of data rate is about 25Mb/s in a room 10m on each side, although higher rates have been demonstrated under particular conditions. Interference from ambient light is a particular issue for diffuse systems because of the extremely wide field view of the receivers.

2.2 THE IRDA STANDARD FOR VERY SHORT DISTANCE POINT-TO-POINT SYSTEMS

An exciting development in recent years has been the arrival of very short distance 'point and shoot' optical wireless systems for laptop computers, PDA's, palmtops, printers, calculators and mobile phones. These wireless systems are commonly referred to as IrDA systems in recognition of the IrDA standard that they embody. The Infra-red Data Association (IrDA) was established in 1993 with the aim of producing an open standard for wireless data communication using mature, commercially available infra-red components. The resulting protocol provides a simple, low power, low cost, reliable means of wireless infra-red communications for a broad range of computing, communications, and consumer devices. The IrDA now has some 160 member companies around the world, and IrDA systems are already resident on over 97% of new portable computers (this includes laptops, PDA's, palmtops, etc).

The IrDA standard presently specifies the following parameters :-

- data rates from 128kbit/s up to 4Mbit/s (raising this upper limit to several 10's of Mbit/s is being considered),
- maximum operating range of 1m (increasing this to 10m is being considered),
- 30 degree cone from the transmitter that equates to a 50cm beam diameter at the receiver positioned 1m away
- very wide receiver field of view.

All of these features ensure that a useful data rate is available over a wireless link that requires only the crudest of alignment.

2.3 OTHER STANDARDS USED IN DIFFUSED INFRARED SYSTEMS

The main importance of standards is to provide wireless connectivity to automatic machinery, equipment or stations that require rapid deployment, which may be portable or hand held or which may be mounted on moving vehicles within a local area. The other importance is to offer a standard for use by regulating bodies to standardize access to one or more frequency bands for the purpose of local communication.

2.3.1 Different IEEE 802 Standards

The IEEE has produced several standards for Local Area Networks. These standards, collectively known as IEEE 802, include CSMA/CD, CSMA/CA, Token bus, Token ring, etc. The various standards differ at the physical layer and Medium Access Control (MAC) sub-layer but are compatible at the data link layer. The IEEE-802 standards have been adopted by ANSI American National Standard, by NIST as government standards, and by ISO as international standards (known as ISO-8802).

The various IEEE standards with applications are mentioned below,

1. IEEE 802.1 standard gives an introduction to the set of standards and defines the Interface Primitives.
2. IEEE 802.2 standard describes the upper part of the data link layer, which uses the LLC (Logical Link Control) Protocol.
3. IEEE802.3 standard describes Ethernet LAN (CSMA/CD) as wire distribution system.
4. IEEE 802.4 standard describes Token bus LAN .
5. IEEE 802.5 standard describes Token ring LAN, Fiber Distribution Data Interface (FDDI), Metropolitan Area Network (MAN).
6. IEEE 802.6 standard describes DQBS Access Method.
7. IEEE 802.7 standard describes Broad band Local Area Networks.
8. IEEE 802.9 standard describes Integrated Services.
9. IEEE 802.10 standard describes LAN/MAN Security.

10. IEEE 802.11 standard describes Diffused IR & RF Wireless Local Area Network.
11. IEEE 802.12 standard describes Demand Priority Access Methods.
12. IEEE 802.15 standard describes Wireless Personal Area Networks.

IrDA standards describes Indoor Point-to-Point Wireless Local Area Networks.

Blue Tooth system: It is the title used for an open-specification system designed to provide a fast and secure short range radio interconnection between portable device and a LAN through the use of spread spectrum techniques using frequency hopping.

2.3.2 Scope of effort of IEEE 802.11 Standard

The scope of effort of IEEE 802.11 standard is to define physical layer wireless data networking and physical layer transmissions (PHY) by radio or Infrared and Medium Access Control (MAC) Protocol compatible with the existing standards for higher layers. The IEEE standard for wireless LAN started in 1988 as IEEE 802.4L as a part of the IEEE 802.4 Token bus wired LAN standard.

In 1990, the IEEE 802.4L changed its name to IEEE 802.11 to form a standalone Wireless LAN standard in the IEEE 802 LAN standard Organization and several draft standards have been published for review. With long effort, the IEEE 802.11 group developed a framework to incorporate wireless specific issues such as power control, frequency management, roaming and PHY and MAC Protocol sub-layer in LAN standards.

The IEEE 802.11 draft standard describes mandatory support for 1 Mb/s Wireless LAN with optional support for a 2 Mb/s data transmission rate. At present there are two emerging wireless LAN standards in use, as mentioned below.

1. European Telecommunication standards institute's High Performance European Radio LAN (HIPERLAN), for data rates up to 23.529 Mb/s.

2. The IEEE 802.11 standard for Wireless LAN.

Both draft standards cover the PHY and MAC sub-layer of the open systems interconnection (OSI) seven layer reference model.

2.4 COMPARISON BETWEEN RADIO AND OPTICAL DIFFUSED WIRELESS SYSTEMS

Recent advances in the radio systems have narrowed the gap between them and indoor optical wireless systems to the point that, in some instances, the optimum choice is not obvious. The commercial indoor optical wireless systems can deliver 4Mb/s (diffuse) and 10Mb/s (line of sight) into a room of some 10m on each side . The technology exists to improve on these rates and cell size, but commercial systems that exploit this have yet to appear. Today's radio (or wireless) LAN systems can deliver 2 Mb/s to multiple users over distances of typically 50-100m depending on the terrain, with the promise of 8 Mb/s in the near future . Standards are being produced for next-generation systems to deliver tens of megabits per second.

Radio systems will almost always afford a greater reach and wider coverage than optical wireless systems because a higher transmitter power can be used and the receivers can take full advantage of sensitive heterodyning techniques. On the other hand, radio will always be a narrower-bandwidth medium than optical, although this is not apparent in today's commercial systems because optical wireless manufacturers have yet to fully exploit the available bandwidth. Optical wireless (tele-point in particular) can deliver high capacity to multiple users within a small cell, whereas radio can produce a much larger cell but will deliver lower capacity. It is therefore easy to envisage scenarios in which both types of system would benefit from being used in combination. For example, a large open plan office would deploy optical tele-point systems to establish several discrete high capacity cells, each spanning a small cluster of perhaps four to six desks; additionally, a single radio system would be deployed to cover the whole office.

The advantages of optical signals over their RF counterparts include a larger potential bandwidth, the use of cheaper transceiver components that enable simple broadband modulation/direct detection techniques, no fading, signal security at the physical layer, and frequency reuse in other parts of the building. One of the drawbacks, however, is that the transmission power is restricted by eye and skin safety regulations. This implies the need for high sensitivity at the receiving end. Two major impairments that are associated with the optical wireless (OW) environment are ambient noise and

multi path dispersion. The difference between radio and infrared are summarized below in tabular form.

Table 2.1 : Properties of infrared and radio channels.

Property	Infrared	Radio
Multi path fading	No	Yes
Multi-path dispersion	Yes	Yes
Source of bandwidth limitation	High photodiode capacitance, multi-path dispersion	Regulatory
Source of dominant noise	Ambient background light	Interference from other users
Security	High	Low
Range	Low	High
Pocket receiver	No	Yes

On balance, the virtually unlimited, unregulated bandwidth of infrared dwarfs its disadvantages, making infrared a promising medium for short-range wireless links. In fact, it may be the only option for cost-effective high-speed communication at rates near 100Mb/s. Of course, infrared networks will not replace radio networks; rather, they will coexist, with radio providing ubiquitous coverage at moderate data rates, and infrared providing short-range, high-speed mobile access where necessary.

CHAPTER 3

DESIGN OF A DIFFUSED INDOOR INFRARED LINK

This chapter gives the system considerations and design of a diffused indoor link. System requirements, performance measures, system constraints and analytical models for predicting the power received at a given point are detailed in this chapter.

3.1 CHOICE OF SYSTEM ELEMENTS

The essential components of a diffused IR link are the transmitter and the receiver. Selection of a suitable source and detector depends on several factors. Similarly one needs to choose an appropriate receiver front end considering the system requirements.

3.1.1 Choice of Source

The two major considerations as far as the source selection is concerned are the power requirements and personnel eye safety. Being an indoor system with diffused radiation laser sources cannot guarantee power levels that are eye safe. Also, laser sources being spatially coherent makes it difficult to obtain diffuse radiation without added optics. Under such conditions the best choice is the LED source which gives out incoherent beam which are eye safe. Unfortunately the output optical power levels are quite low for single LED sources. Hence an array of LEDs will have to be used to achieve diffused radiation within a room. In addition to the power output requirements another very important parameter is the required optical beam parameters of the source. Ideally sources for diffused applications must have omni-directional patterns making it possible to radiate power equally to all corners of the room. This is a real challenge. In our study transmitters were made using both single LED as well as an array of LEDs.

The wavelength of operation of the LEDs is another design consideration. Because of the advances in fibre optic systems, LED and laser diode optical sources are available at 850nm, 1300nm and 1550nm. Considering the cost as well as the available output powers AlGaAs or GaAs sources emitting light in the range of 820-900nm are the ideal sources. They have the added advantage that silicon detectors have maximum

response at these wavelengths. Hence 850nm is the most preferred wavelength. In our design wavelength of 820nm was used.

3.1.2 Choice of Detector

Another major element is the photodetector for the optical receiver. The choice of photodetector depends mainly on the two factors, viz. The response time and the sensitivity of the receiver system. The upper limit of the permissible response time is determined by the accuracy required and/or the modulation bandwidth of the receiver signal. The response time in the range 1-100ns are generally required. The silicon PIN photo diode is the recommended detector for most of the IR communication systems. Such a detector works best when reversed biased. The photocurrent produced by a PIN detector is directly proportional to the incident light power level (light intensity). At 900nm the typical responsivity of a silicon detector is 0.6 Amps/Watt. The responsivity relationship of a detector is independent to the size of the detector. The PIN photo diode size should be chosen based on the required frequency response and the desired acceptance angle with the lens being used. Large PIN photodetector will have slower response times than smaller devices. For example, 1cm x 1cm diodes should not be used for modulation frequency beyond 200 kHz, while 25mm x 25mm diodes can work beyond 50MHz. If a long range is desired, the largest photo diode possible that will handle the modulation frequency should be used.

Two types of detectors have been generally used, PIN photodiodes and Avalanche photodiodes. Both these detectors find extensive use in fibre optic and IR systems. The real job of the light detector is to convert light power into electrical power, independent of the energy of the transmitted light pulses. This relationship also implies that the conversion must be independent of the duration of the light pulses used. This is an important concept and is taken advantage of in many of the systems. This device is most sensitive to the near infrared wavelengths at about 900nm. Most IR light emitting diodes (IR LEDs) do indeed emit light at or near the 900nm peak, making them ideal optical transmitters of information.

The PIN photo detector behaves very much like a small solar cell or solar battery, which converts light energy into electrical energy. Like solar cells, the PIN photo diode will produce a voltage (about 0.5v) in response to light and will also generate a current proportional to the intensity of the light striking it. However, this unbiased current sourcing

mode, or “photo voltaic” mode, is seldom used in through-the-air communication since it is less efficient and is slow in responding to short light flashes. The most common configuration is the “reversed biased” or “photo conductive” scheme.

It is important to note that the intensity of a light source is defined in terms of power, and not energy. When detecting infrared light at its 900nm peak response point, a typical PIN diode will leak about one milliamp of current for every 2mw of light striking it (50% efficiency).

All PIN diodes have dark current ratings. This rating corresponds to the residual leakage current through the device, in the reversed biased mode, in the absence of any light falling on it. This leakage current is usually small and is typically measured in nano amps, even for large area devices. As one expects, large area devices will have larger dark currents than small devices. Dark currents introduce extra noise into the receivers. In most of the applications the signal current to dark current ration is very large thus making the effect of dark current negligible.

The choice between the APD and PIN photo diodes will often be made on the basis of the cost versus the value of the higher sensitivity normally available from the APD photo detector. Some of the important factors to be considered in the choice between APD and PIN photodiodes are listed below.

- Signal to noise ratio is poor for APD than that of the equivalent PIN photo detector.
- APD photo detectors will have higher sensitivity than a PIN photo detector. Some types of APD have higher dark currents than the corresponding PIN device; In digital receivers this higher noise in the “no optical signal present “ condition will increase the probability of error. The APD requires a substantially higher bias voltage.
- It is the appropriate choice when the advantages it offers are needed, but the PIN is usually preferable if its characteristics are adequate for the system under consideration.
- PIN photo detectors are 20 times less expensive than APDs.
- The additional noise produced by the ambient light focused on to the device cancels much of the gain advantage the APD might have had over a PIN.

- Still, as the technology improves, low cost APDs with large active areas may become available.

3.1.3 Choice of Receiver Front-end

The receiver in an IR link is very similar to that in a fibre optic system. There are basically three types of receiver front-end (preamplifier) configurations available to the designer, viz. low impedance, high impedance and transimpedance front ends. Each one has its own merits and demerits. These front-ends need to be compared from the point of view of their sensitivity, bandwidth and dynamic range. Sensitivity is defined as the minimum optical power required at the receiver for a specified performance and data rate. Dynamic range specifies the range of power over which the receiver is able to function as per specifications. It is generally expressed in decibels as the ratio of the maximum optical power to the minimum power incident on the receiver giving the specified performance.

Low-impedance Front-end:

This type of a front-end is the simplest one where a very low resistance, of the order of 50 or 100 ohms, is used as the photodetector load resistance. The voltage developed across the low resistance is indeed the preamplifier output. This scheme has the advantage that the RC time constant is very small and hence this simple scheme can work up to very high frequencies. Its dynamic range is also large. However, the low load resistance results in very large thermal noise and hence its sensitivity is very poor. This configuration is useful only when the optical signal levels are very large.

High-impedance Front-end

This type of receiver also uses an open loop approach and has a very simple configuration where the detector load resistance is made very large. Due to the large load impedance the bandwidth of this receiver is very low. Hence the preamplifier stage must be followed by an equalization stage to compensate the low-pass behaviour of the front-end. This type of front-end has the advantage that the thermal noise generated by the load is very low. However, its dynamic range is very low because of the overloading due to large impedance. Due to its poor dynamic range and bandwidth, this type of a receiver front-end is used only when noise performance is the main criterion.

Transimpedance Front-end

Transimpedance front-end is a good compromise between the low and high impedance ones. This type of a front-end utilizes a feedback amplifier with a feedback resistor large enough to reduce noise and at the same time lower than that used in high impedance design to improve bandwidth.

3.2 LIMITATIONS OF THE SYSTEM ELEMENTS

The performance of a diffused IR link is affected by some of the inherent limitations of various system elements. These arise out of the limitations of the LED as a source, poor receiver sensitivity and also the presence of ambient light.

The use of LED sources for eye safety puts serious limitations on the output optical powers. Power output of single LED sources is too small to illuminate a given area. This problem can be solved to some extent by the use of an array of LEDs.

In order to have large coverage range the receiver used in the IR link should have very good sensitivity. Due to cost and other factors PIN photodetector is the common choice as a detector. The sensitivity achievable with receivers made of PIN detectors may not be sufficient for indoor IR systems and hence one has to be satisfied with typical values of receiver sensitivity. Under such conditions range can only be improved by increasing LED output power and by reducing all other sources of noise.

Another serious problem in indoor IR systems is the presence of ambient light. This will lead to extra noise due to unwanted light. This problem can be solved to a large extent by using a narrow band filter in front of the receiver. In our study the ambient lighting was kept to a minimum due to the non-availability of suitable light filters.

3.3 MEASURES OF SYSTEM PERFORMANCE

The major measures of the performance of an IR link are its data rate, maximum coverage range and error rate. IR links are capable of transmitting and receiving data in excess of a few Mbits/sec. However, diffused links suffer from dispersion due to multipath propagation. In our study our aim was to design an IR link capable of transmitting about 1 M bts/sec. However, our receivers worked well only up to about 300 kbits/sec.

Another major parameter of an IR link is its coverage range. Since LEDs are used as the optical sources it is very difficult to achieve long ranges due to their limited power outputs. However, by using multiple sources in the form of an array of LEDs the output powers can be increased to a large extent. In addition to the output power another important source parameter from the point of view of range is the optical beam profile of the sources. In diffused links the sources should emit light in all directions. This is not possible by individual semiconductor optical sources as they have finite intensity beam profiles, typically of the form, $I(\theta) = I_0 \cos^n \theta$. Beams such as the above have maximum intensity along the axis and the intensities decrease drastically with θ . Thus in order to make the optical beams made up of such sources close to an omni-directional one, it is necessary to use multiple LEDs arranged in some fashion. Some such LED array arrangements have been studied by us and their effect on the beam profile also has been studied.

The error rate performance of an IR link can be measured using a standard Bit Error rate measurement system. As such a system was not available to us the received data and displayed along side the transmitted one on a CRO and then compared.

3.4 THEORETICAL MODELS FOR PREDICTION OF OPTICAL POWER AT A POINT

In the design of an IR link it is important to be able to predict the optical power as a function of the distance from the source. However, this is a very difficult task and to the best of our knowledge the literature is silent on this issue. We have applied some of the models used in related areas (power coupling from optical sources to fibres and detectors) and modified them for predicting power levels in the longitudinal direction (with the source and detector axes aligned). These models are presented below with theoretical results. These results are later compared with experimental data in Chapter 4.

3.4.1 Power Transfer Model from a Radiating Surface with Angular Distribution (Model-1)

The power transfer from a radiating surface to a receiving surface can be obtained if the goniometric characteristics of the two surfaces are known. Fig.3.1 gives an arbitrary

orientation of radiating and receiving surfaces where A_S is the radiating surface area and A_R the receiving surface area. Let the separation distance between these surfaces be the distance vector r_{SR} , as shown in Fig.3.1. The power transfer from an element of area dA_S to an element of area $\cos \theta_R dA_R$ normal to r_{SR} is given by

$$dP_{SR} = B_{\Omega} (X_S, \theta_S) dA_S \cdot d\Omega_R \quad (3.1)$$

where $B_{\Omega} (X_S, \theta_S)$ is the brightness of the source in units of watts per square centimeter steradian. For sources with non-uniform radiation distributions, B_{Ω} is a function of X_S which is the position vector on the surface A_S .

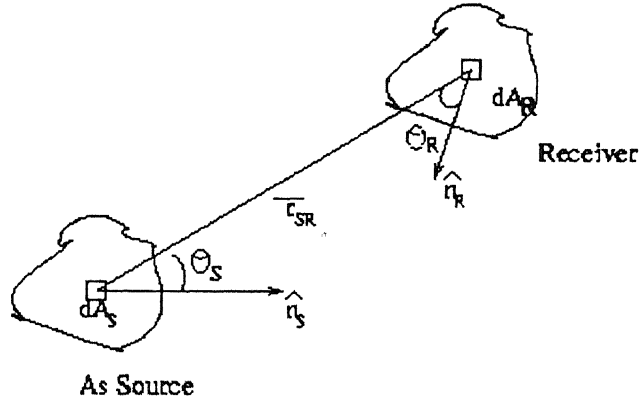


Fig.3.1 Arbitrary orientation of emitting and receiving surfaces.

The quantity $d\Omega_R$ is the solid angle subtended by $(\cos \theta_R dA_R)$ at the source point dA_S , that is ,

$$d\Omega_R = \cos \theta_R dA_R / r_{SR}^2 = \text{projected area} / \text{square of distance} \quad (3.2)$$

The total power transfer between A_S and A_R is , therefore,

$$P_{SR} = \int_{A_S} \int_{A_R} B_{\Omega} (X_S, \theta_S) \cos \theta_R r_{SR}^{-2} dA_S \cdot d\Omega_R \quad (3.3)$$

In general, this integral is complicated with the angle θ_S and θ_R and the separation vector r_{SR} being dependent on the position coordinates on the surfaces A_S and A_R . In the interest of obtaining an estimate of power coupled, approximations can be made which considerably simplify the integration.

From the two arbitrarily oriented differential surface areas shown in Fig.3.2 we see that the area $dA_R \cos \theta_R$, which is normal to the vector r_{SR} is the sphere centered at

dA_S , i.e $dA_S \cos \theta_R \cong r_{SR}^2 \sin \theta_S d\theta_S d\phi$. The angle ϕ is an angle varying from 0 to 2π in the source plane. The total power transferred between A_S and A_R is, therefore

$$P_{SR} = \int_{A_S} \int_{\theta_S} \int_{\phi} B_{\Omega} (X_S, \theta_S) \sin \theta_S d\theta_S d\phi. dA_S \quad (3.4)$$

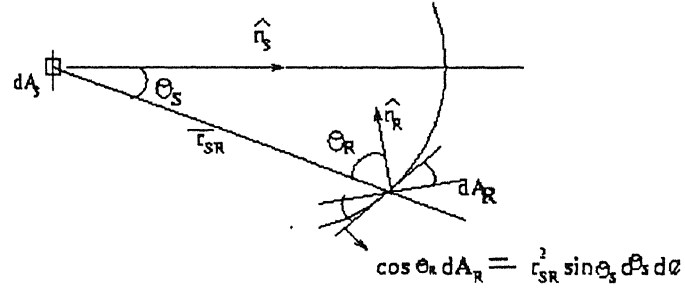


Fig.3.2 Arbitrarily oriented differential surface areas dA_S and dA_R

Assuming that the source has uniform radiation distribution across its area and that the source has a uniform radiation distribution across its area compared with the separation vector r_{SR} , the total power transfer becomes

$$P_{SR} = 2\pi A_S \int B(\theta) \sin \theta d\theta \quad (3.5)$$

The external radiant intensity from a planar geometry surface-emitting LED is the same as a planar radiating surface with brightness value

$$B(\theta) = B_0 \cos^n \theta \quad (3.6)$$

Substituting,

$$P_{SR} = 2\pi A_S \int B_0 \cos^n \theta \sin \theta d\theta \quad (3.7)$$

$$= 2\pi A_S B_0 \left[(1 - \cos^{n+1} \theta_S) / (n+1) \right] \quad (3.8)$$

The total optical power emitted from the source into the full hemisphere is given by

$$\begin{aligned} P_S &= 2\pi A_S \int_0^{\pi/2} B_0 \cos^n \theta \sin \theta d\theta \\ &= 2\pi A_S B_0 / (n+1). \end{aligned} \quad (3.9)$$

The power received by the receiver is given by

$$\begin{aligned}
 P_R &= 2\pi A_S \int_0^{\theta_{\max}} B_o \cos^n \theta \sin \theta d\theta \\
 &= 2\pi A_S B_o \left[(1 - \cos^{n+1} \theta_{\max}) / (n+1) \right]
 \end{aligned} \tag{3.10}$$

Power coupling efficiency, from source to the receiver is then given by

$$\eta = P_R / P_S = A_R / A_S \left[1 - \cos^{n+1} \theta_{\max} \right] \tag{3.11}$$

$$\text{If } A_R \gg A_S \text{ then } \eta = 1. \tag{3.12}$$

Except when the receiver is situated very close to the source, $A_R \ll A_S$ and hence eqn. (3.11) holds.

The source pattern in the above power transfer model was considered to be of the form given in eqn.(3.6). In our study we observed the LED far field patterns to have shapes very similar to that of eqn.(3.6). This equation is plotted for some values of n and is given in Fig.3.3. A special case of the above source pattern is when $n=1$, in which case $B(\theta) = B_o \cos \theta$. Such sources are called Lambertian sources. Point sources are expected to have Lambertian beam profiles.

Variation of optical power as predicted by the above model is plotted in Fig.3.4 for some values of n . These results will be compared with the measured results in Chapter 4.

3.4.2 LED Source to Receiver Power Transfer Assuming Uniform Power

Distribution (Model-2)

This is a simple model based on geometry of the source and the receiver where the LED source is assumed to be emitting light in a cone and reaching the receiver having a finite area. The mismatch between the projected source and receiver areas give a measure

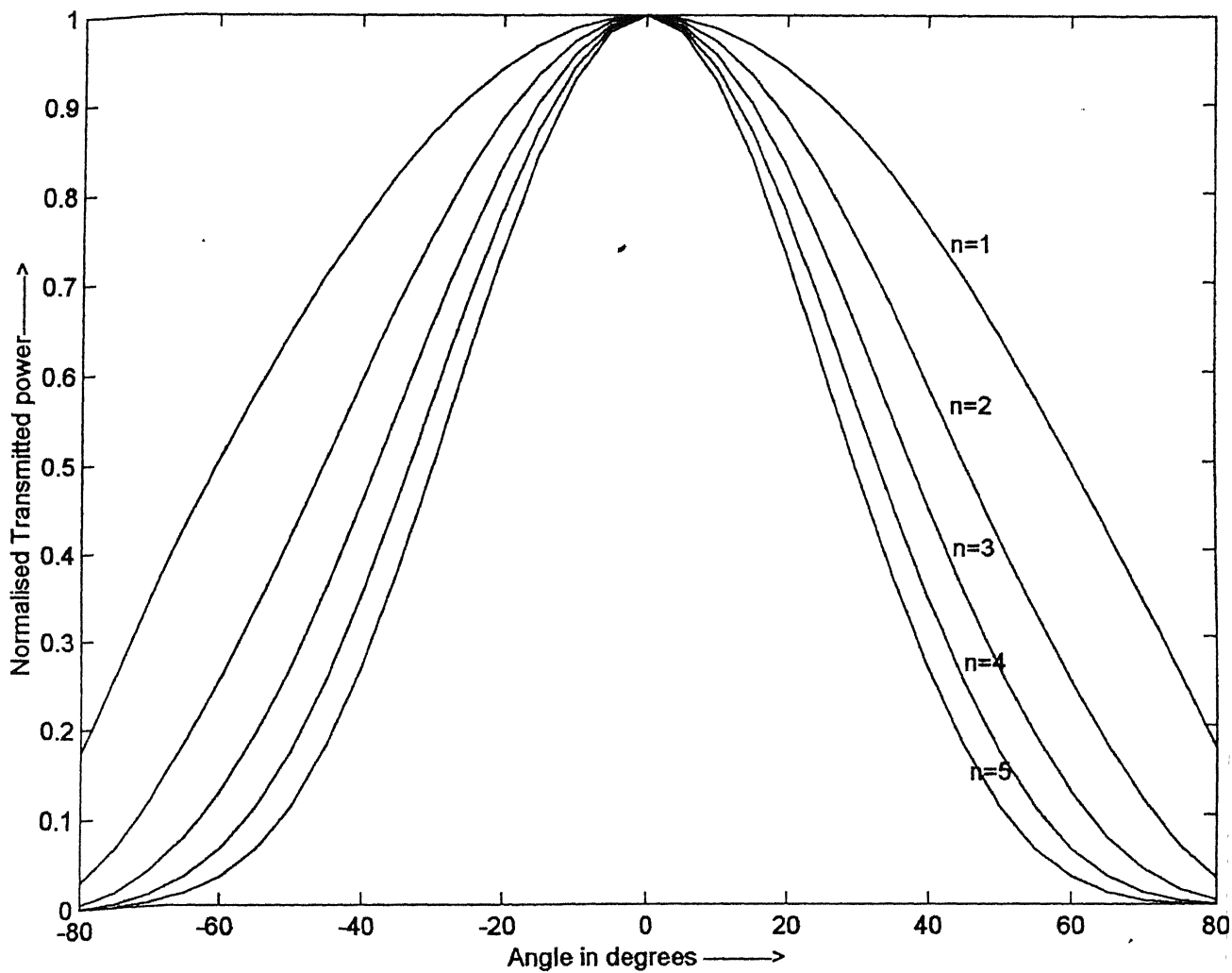


Fig 3.3 $B(\theta)$ patterns for Different n values

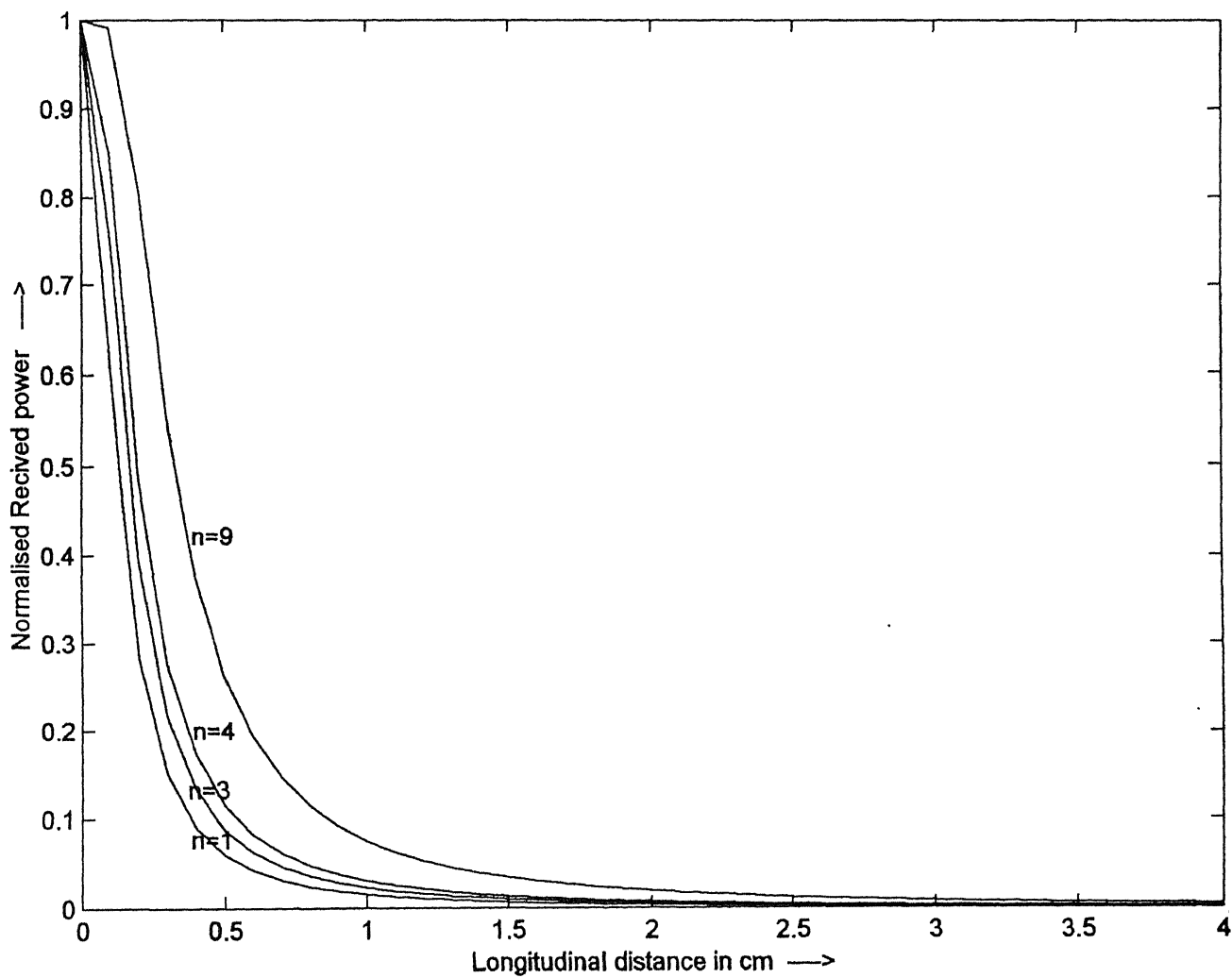


Fig3.4 Norm. Variation of Power as a function of distance

of the power transfer from source to the receiver. The power distribution within the source cone is assumed to be uniform. Fig.3.5 illustrates the source and receiver geometries for this model.

With reference to Fig.3.5, the radius of the circular spot is given by,

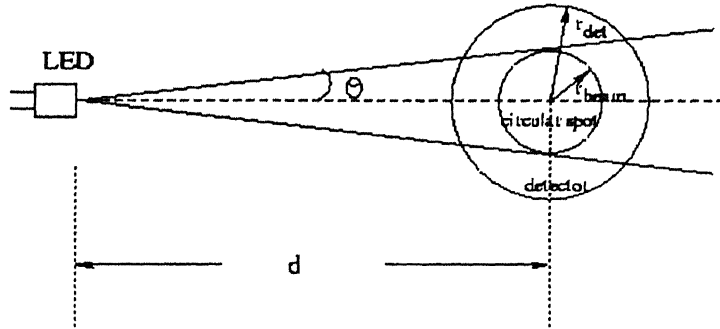


Fig.3.5 Uniform power distribution.

$$\tan \theta = r_{\text{beam}} / d, \text{ or } r_{\text{beam}} = d \tan \theta \quad (3.13)$$

where r_{beam} is the radius of the beam, θ is the angle subtended by the detector at the source and d is the distance of the receiving surface from the source LED.

Power coupling efficiency (η) at various longitudinal offsets can be calculated assuming the lateral offsets to be zero. There are two distinct cases, depending on the radius of the beam (r_{beam}) and the radius of the detector (r_{det}).

Case 1 : $r_{\text{beam}} < r_{\text{det}}$

$$\eta = 1.0 \quad (3.14)$$

In this region since all the power falls within the detector area and hence $\eta = 1.0$.

Case 2 : $r_{\text{beam}} > r_{\text{det}}$

For this case η is the ratio of the area of the detector to that of the beam.

$$\begin{aligned} \text{i.e. } \eta &= \text{Area of detector} / \text{Area of beam} \\ &= (\pi r_{\text{det}}^2) / (\pi r_{\text{beam}}^2) \end{aligned}$$

$$= (r_{\text{det}} / r_{\text{beam}})^2 \quad (3.15)$$

Substituting $r_{\text{beam}} = d \tan\theta$ we get

$$\begin{aligned} \eta &= r_{\text{det}}^2 / d^2 \tan^2\theta \\ &= k / d^2 \end{aligned} \quad (3.16a)$$

$$\text{where } k = r_{\text{det}}^2 / \tan^2\theta \quad (3.16b)$$

This the coupling efficiency as per this model is inversely proportional to the square of the longitudinal offset.

In this model one very important parameter is angle θ of the emitting cone. For different values of θ , the coupling efficiencies will be different. The above model assumes uniform power within the circular cone formed by the emitting beam which is not actually true. However, an effective cone angle may be used in the expression of eqn.(3.16) to arrive at the coupling efficiency. Normalised variation of optical power along the axis as a function of separation distance d for various values of θ is plotted in Fig.3.6.

3.4.3 LED Source to Receiver Power Transfer Assuming LED beam to be Gaussian (Model-3)

Because of the simplicity in describing mode field distributions as Gaussian, the same is very commonly used to describe beam profiles, especially for describing Laser beams. Even though it is incorrect to use Gaussian beam approximation incoherent LED beams, it was observed from our study that the far-field pattern of LEDs had a nearly Gaussian intensity variation with θ . This compelled us to try some of the standard results available for Gaussian beams for the present study in predicting the variation of optical power with axial separation distance between the source and the receiver. In this section, we briefly discuss the fundamental Gaussian beam features followed by a Gaussian fit for LED source far field patterns.

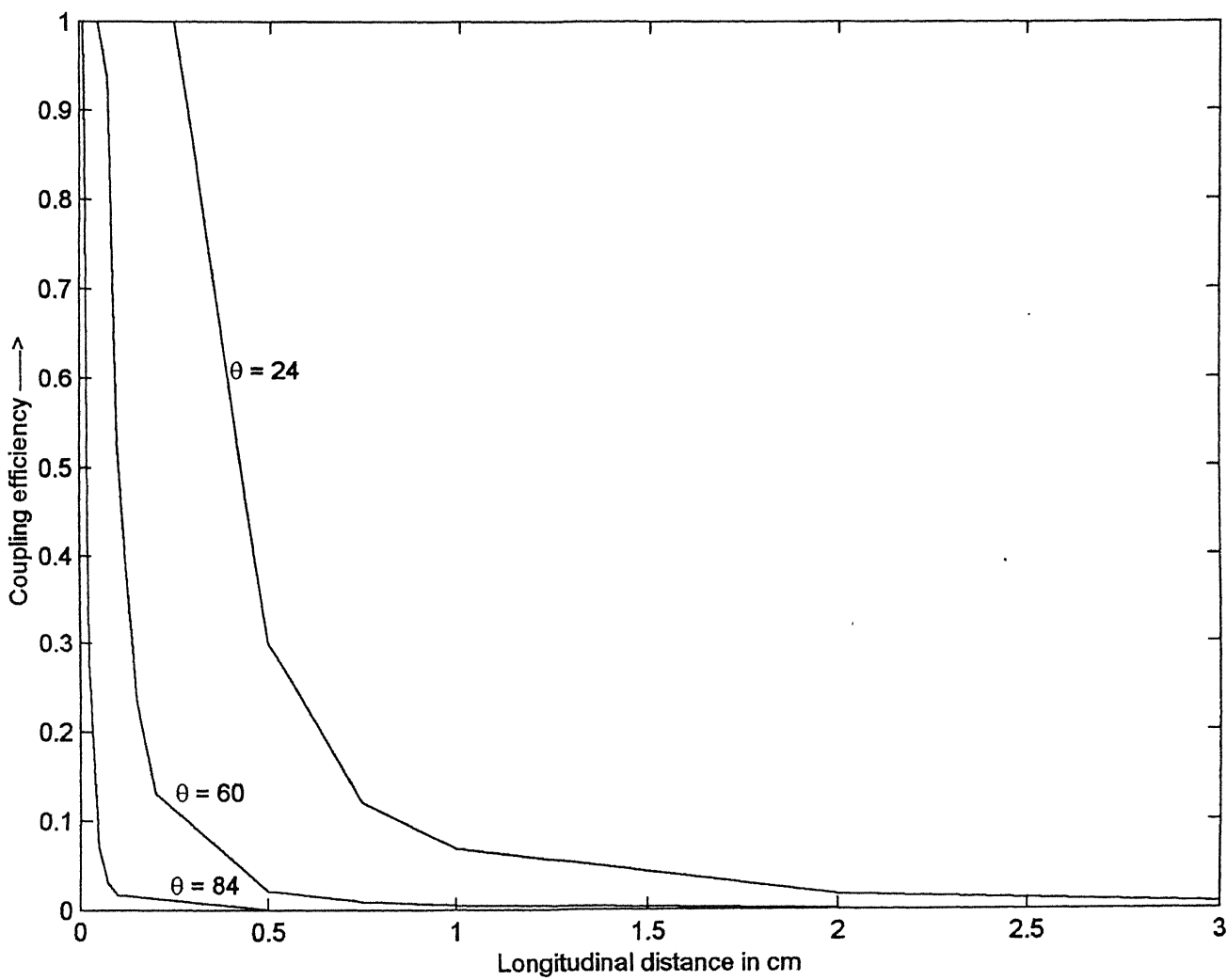


Fig 3.6 Coupling efficiency for different θ values of the cone

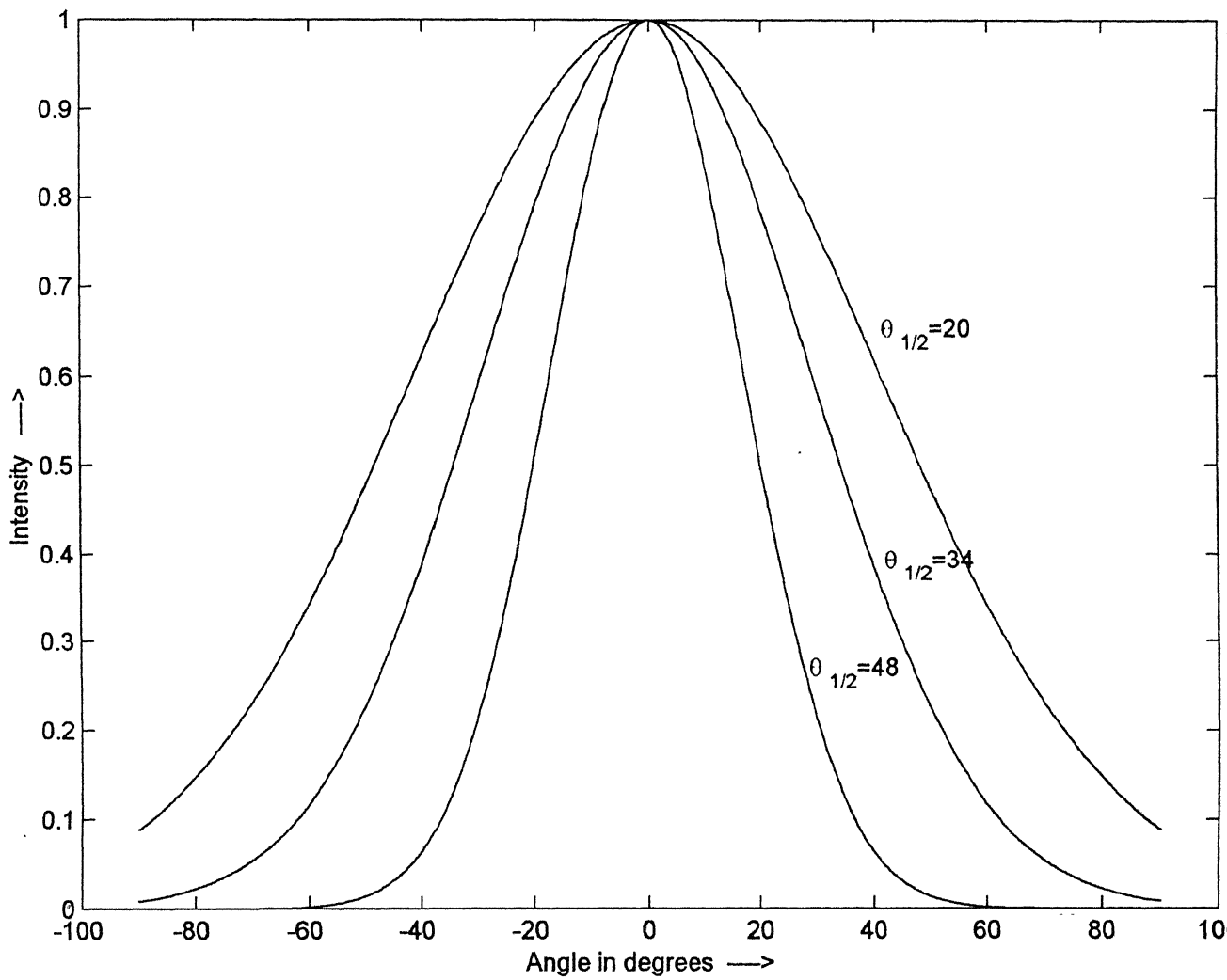


Fig3.7 Gaussian Far field patterns

3.4.3.1 Properties of fundamental Gaussian Beam

The field equation for the fundamental Gaussian beam can be written as

$$U(r,z) = (w_0/w) \exp(-j(kz - \phi) - r^2((1/w^2) + ik/2R)) \quad (3.17)$$

where $R(z)$ and $w(z)$ are the radius of curvature and spot-size of the beam respectively and are given by

$$R(z) = z \{ 1 + (kw_0 / (2z))^2 \} \quad (3.18)$$

$$w^2(z) = w_0^2 \{ 1 + (2z / (kw_0^2))^2 \} \quad (3.19)$$

In the above expressions, w_0 is called the waist spot-size. $R(z)$ is the radius of curvature of the wave front that intersects the axis at z , and $w(z)$ is a measure of the decrease of the field amplitude with distance from the axis. 'w' is the distance at which the field amplitude is $1/e$ times that on the axis, and is called beam radius or spot size of the beam.

A single Gaussian fit for the far-field intensity pattern, perpendicular to the emitting plane was suggested by Boetz, which takes the form.

$$I(\theta) = \exp(-0.69 \theta^2 / \theta_{1/2}^2) \quad (3.20)$$

where $\theta_{1/2}$ is the half width of the far-field pattern when $I(\theta) = 0.5$. In our studies the far field patterns of different LEDs were measured experimentally and a Gaussian fit was obtained in each case using the corresponding half angle $\theta_{1/2}$. Gaussian intensity distributions for a few half angle are plotted in Fig.3.7.

Assuming the source output to be Gaussian, one can estimate the power coupled from the source to the receiver located at an axial distance.

3.4.3.2 Power Received for Finite Longitudinal Offsets

Assuming the offset between the source and receiver to be only longitudinal (axial) the power received at the detector can be calculated knowing that it is proportional to the overlap area between the beam and detector. Neglecting phase shifts the Gaussian beam expression of eqn.(3.17) reduces to

$$I(r,z) = (w_0 / w(z)) \exp(-r^2 / w(z)^2) \quad (3.21)$$

Because of the symmetry of the problem eqn.(17) can be written in one dimension for the sake of simplicity as

$$I(x,z) = (w_0 / w(z)) \exp(-x^2 / w(z)^2) \quad (3.22)$$

The power coupled to the detector can be simply calculated by the overlap of the Gaussian beam on the detector's area.

Power coupled to the detector, P_D is given by

$$P_D = 2 \int_0^{r_{det}} I(x,y) dx = 2 \int_0^{r_{det}} (w_0 / w(z)) \exp(-x^2 / w(z)^2) dx \quad (3.23)$$

Total power emitted by the LED is given by, P_S

$$P_S = 2 \int_0^{\infty} \exp(-x^2 / w_0^2) dx = (\pi)^{1/2} w_0^2 \quad (3.24)$$

From the above the coupling efficiency from source to detector is obtained as

$$\eta = P_D / P_S \quad (3.25)$$

Hence the power at the receiver can be obtained as $P_D = \eta P_S$.

The expression for P_D is complicated and hence cannot be obtained analytically. Numerical integration needs to be done to obtain η . In our present work the Gaussian model was not explored further.

SYSTEM IMPLEMENTATION AND PERFORMANCE

This chapter gives the implementation details of the diffused IR link tried out by us. As discussed earlier in order to achieve large range the optical power output of the source should be as high as the eye safety limits would permit. For indoor systems the only permissible sources are LEDs. We used single LEDs as well as multiple LEDs in our implementation.

4.1 LED SOURCES

The LED sources used in our system were commercial IR LEDs, used for remote control applications in TVs emitting light at about 820nm. Though driver circuits based on single LEDs are easy to implement, their limited power outputs will affect the range of data transmission considerably. We used transmitter circuits making use of both single LEDs as well as circuits with three LEDs.

4.1.1 Measurement of Source Characteristics

The two major source characteristics that are important in wireless IR communications are current-intensity (optical power) and the far-field characteristics. The former would give an idea about the drive current currents for a given power and is hence critical in the driver circuit design. The far-field characteristics however give an idea about the optical beam profile which determines the directivity of the source.

Measurement of Current – Intensity Characteristics

A simple setup was used to measure the current-intensity characteristics of the source. The setup is shown in Fig.4.1 and the measured characteristics in Fig.4.2. It is seen that the measured relationship between LED current and its optical power is almost linear. It was not possible to measure the LED output at currents higher than 20mA as the LED optical power was well excess of several milliwatts, which was beyond the capability of the power meter and the large area detector available in the laboratory.

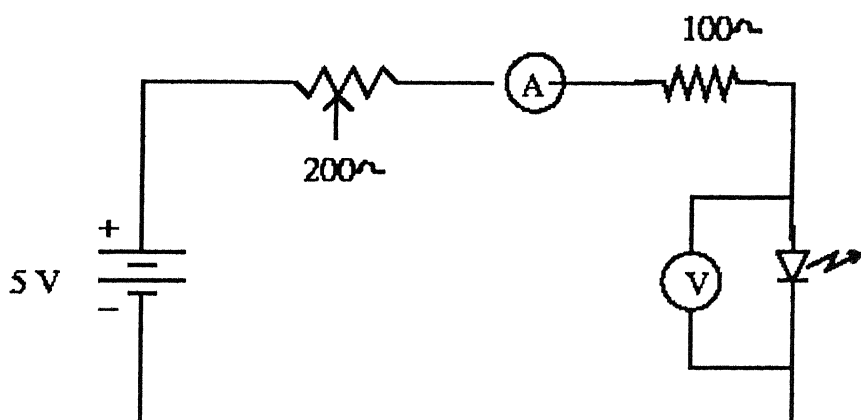


Fig 4.1. Current – Intensity Characteristics Set up

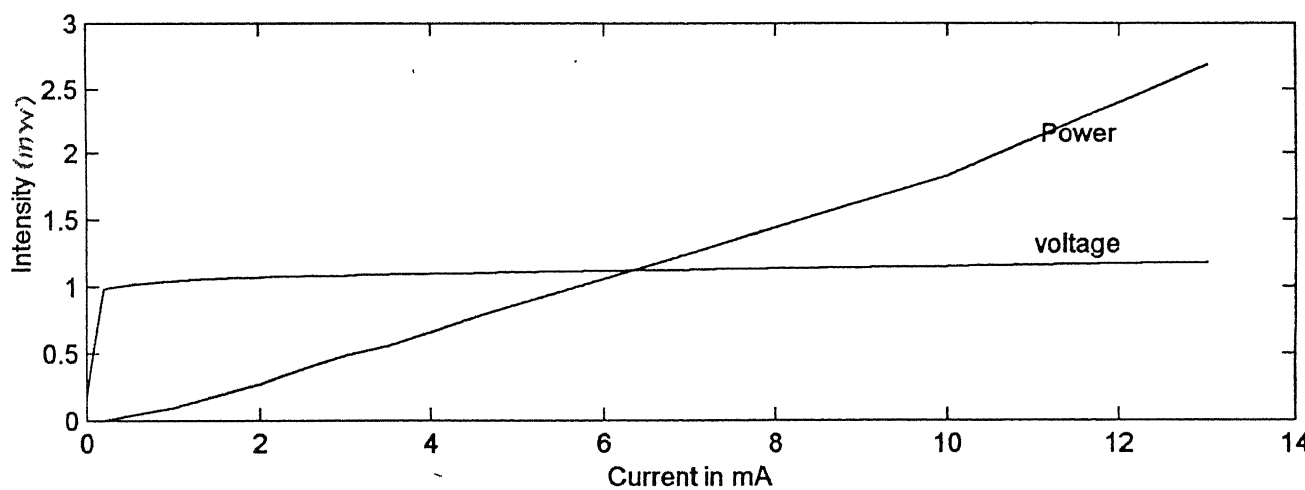


Fig 4.2 Current-Intensity Characteristics results

Measurement of Far field Pattern

The block diagram of the setup used for the measurement of the far-field pattern is shown in Fig.4.3. Different types of LEDs were used in the experiment, viz. round type, cut type and an array of LEDs. Even though the current-intensity characteristics of the LEDs used in this study are similar their far-field patterns may be different. This is especially the case with LED arrays.

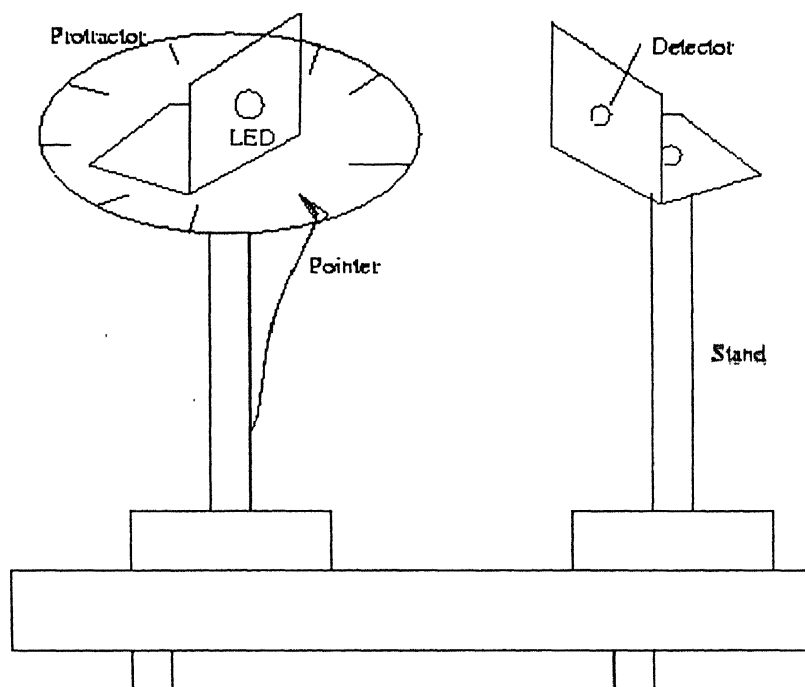
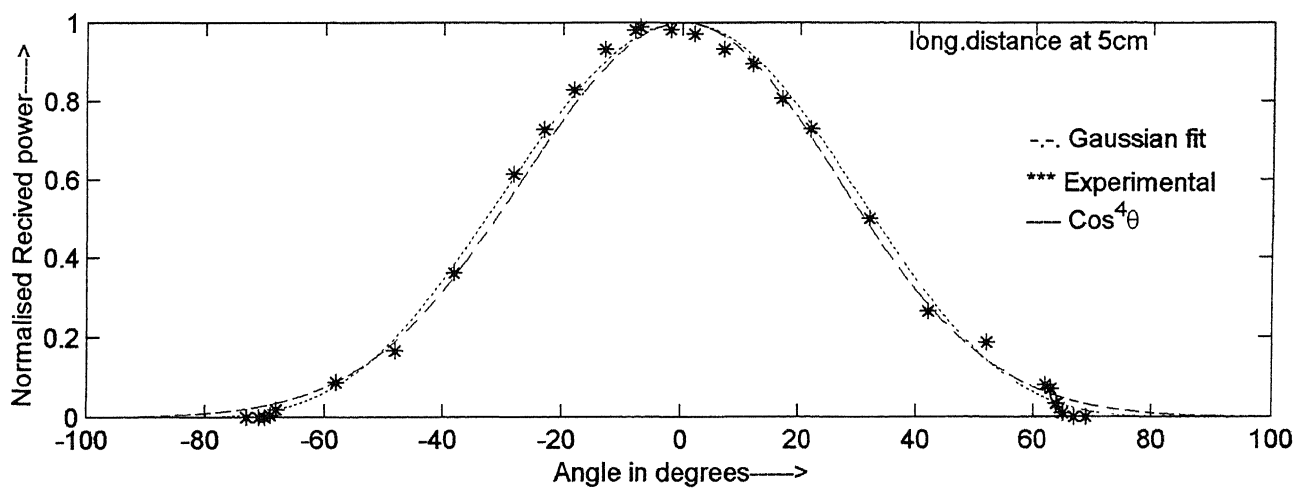
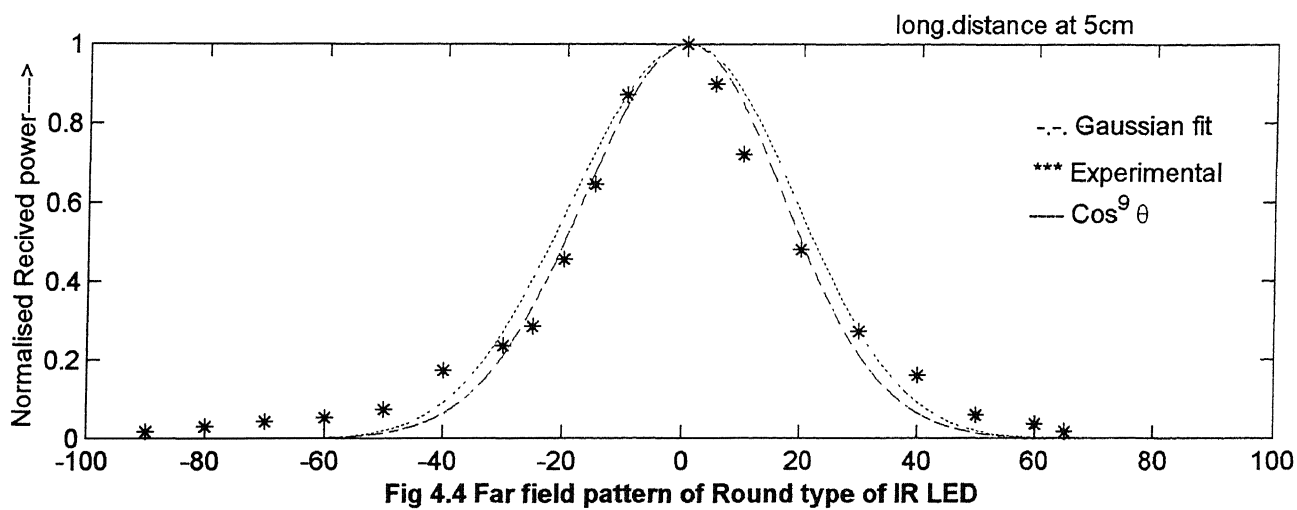


Fig 4.3. Far field measurement set up

In the set up of Fig.4.3, the LED source is fixed at the centre point on the protractor and it is rotated in either clockwise or anti-clockwise direction. A pointer is fixed near the protractor to read the angles at various positions. The detector is kept at a distance of about 5cm from the source and then aligned for maximum power. The detector will receive maximum power when the axes of both detector and source are aligned. The source is rotated thereby misaligning the axes and the power levels at the detector for various angles are noted.



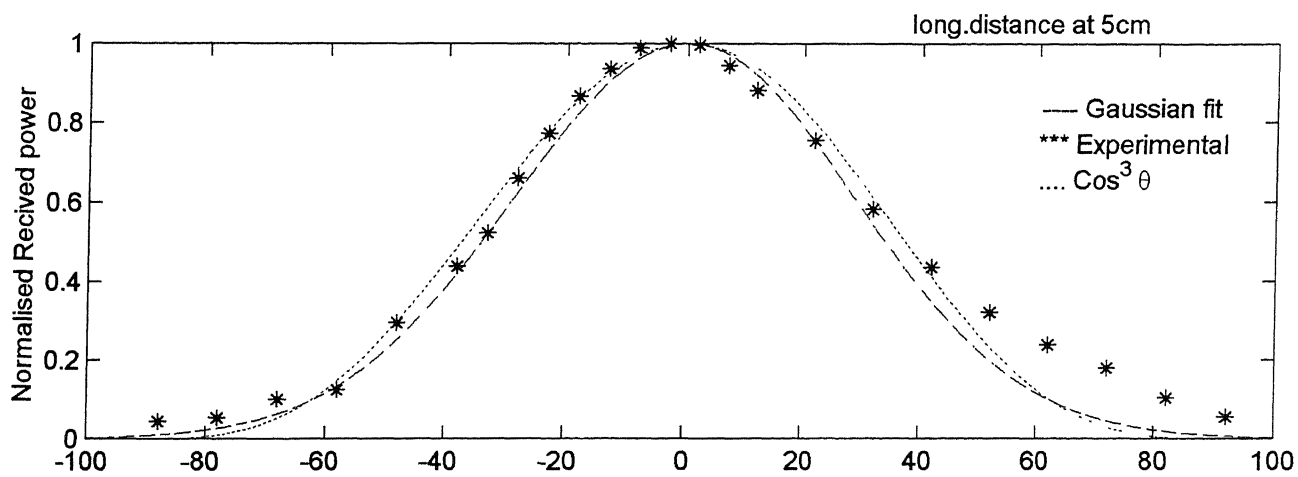


Fig 4.6 Far field pattern of array(3nos) of IR LED

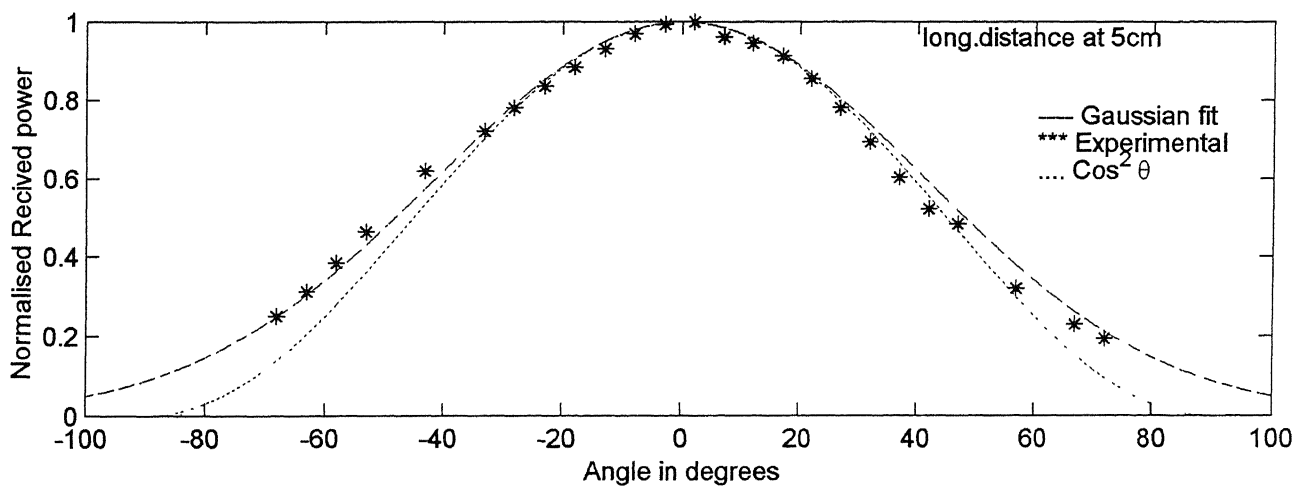


Fig 4.7 Far field pattern of array(5nos) of IR LED

The measured results for single LEDs and LED arrays are plotted in Fig.4.4 - Fig.4.7. Gaussian fits and also the fits assuming the intensity pattern to be of the form $I(\theta) = I_0 \cos^n \theta$ are also given for the best value of n in each case. The gaussian fits were obtained using expression $I(\theta) = \exp(-0.69 \theta^2 / \theta_{1/2}^2)$, where θ is the far-field angle in degrees and $\theta_{1/2}$ the half angle. Half-angle is defined as the angle at which the intensity of the far-field pattern decreases to half of the maximum. A commonly used measure of the half-angle is FWHM (full width at half maximum), which as per the definition is twice $\theta_{1/2}$.

The difference in the far-field patterns are very evident from the above figures. Fig.4.4 is that of a normal LED whereas Fig.4.5 is that of a similar LED whose front curved portion has been removed by lapping. The half-angle of the normal LED (round) was found to be about 20 degrees. It may be observed that the half-angle of this cut-type LED is almost 11 degrees more than the one with a curved front surface.

Fig.4.6 and Fig.4.7 gives the far-field patterns of LED arrays. In the first case three normal LEDs (with curved surfaces) were fixed at the vertices of an equilateral triangle with a distance of ..1 cm. In the latter case five LEDs (with curved surfaces) were fixed on a hemispherical surface of radius ..1 cm as shown in Fig.4.8. It is interesting to note the change in the half-angle of these array LEDs in comparison to single LEDs. The half-angle increased to 34 degrees for the three-LED array, whereas it increased to 48 degrees for the five-LED array. Thus the latter array is found to approach a Lambertian pattern.

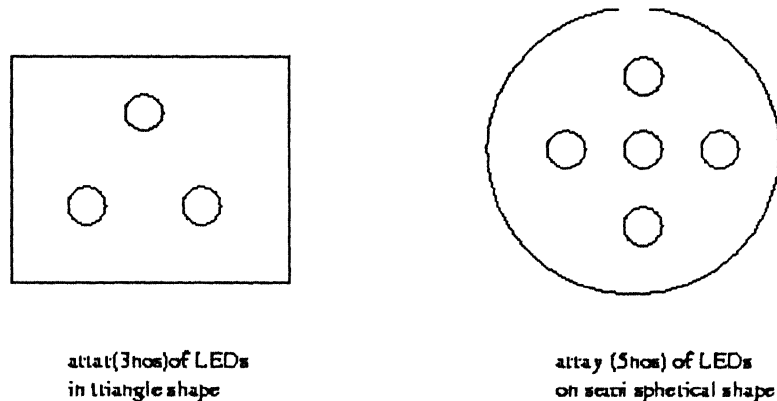


Fig 4.8 .Arrangement of LEDs in the array LED sources.

4.2 PSEUDO RANDOM BIT SEQUENCE (PRBS) GENERATOR

The diffused IR link was tested using a PRBS data generated using a 4-bit shift register. 74F194 Universal shift register was used for this purpose. This shift register is fully synchronous with all operations taking place in less than 20ns (typical). The IC 74F194 has special logic features which increase the range of application. The operation of the device is determined by two mode select inputs, S_0 and S_1 . The functions available with these mode select inputs are right-shift, left-shift, parallel load and hold. The circuit diagram of the PRBS generator is shown in Fig.4.9. In our circuit the shift register was configured in the right-shift mode. It is important to prevent the all zero state in a PRBS generator as such a state would lock itself thereby preventing the generator from generating the PRBS data. In our circuit an auto start circuit consisting of three OR gates from a 74S32 IC and a NOT gate from a 74F04 IC. Under normal conditions (for non zero states) the output of the NOT gate would be a logical '0' which is connected to the S_1 mode input which will give a right shift operation with $S_0 = '1'$. When all zero state is detected the NOT gate output will become '1' thereby forcing the shift register to be in the parallel load mode. A non-zero state '1100' is applied to the data inputs (D_3 - D_0) which will be then loaded and the shift register will thus be able to work normally after that. The output of the PRBS generator was used as data in all our experiments and applied to the input of the transmitter circuit.

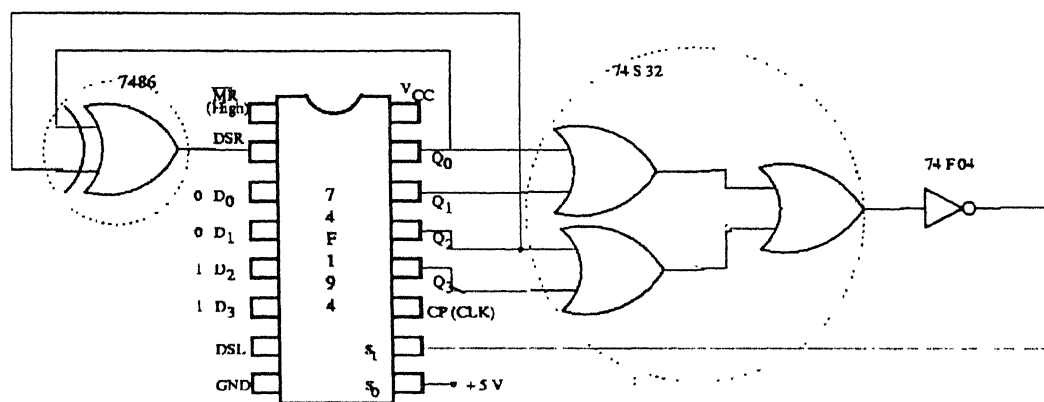


Fig 4.9. PRBS generator circuit.

4.3 TRANSMITTER CIRCUIT (Driver Circuit)

The LED driver circuit is shown in Fig.4.10. The input signal to the circuit was taken from the PRBS generator output at a frequency. The major component of the transmitter is the 74LS140 50 ohm line driver IC. A standard TTL gate can only source $400\mu\text{A}$ and sink 16mA . These values are very low for LED driver applications. In contrast each gate of the 74S140 driver can source 40mA and sink 68mA , which are quite large for most of the applications. In our case two gates of the 74S140 were connected in parallel to get current well in excess of 80mA . The driver IC was used in the sink mode thus turning the LED ON when the gate output is at '0'. Since the IC uses NAND logical function the LEDs turned ON when the input to the gate was at logical '1'. In the sink mode the drop across the LED and resistance worked out to be $V_{CC} - V_{OL}$ i.e. $5 - 0.2 = 4.8\text{V}$. The forward drop of the LED was about 1.75V . Hence it was possible to cascade up to 2 LEDs using the same transmitter as shown in Fig.10(b). This reduced the circuit complexity for transmitters using LED arrays.

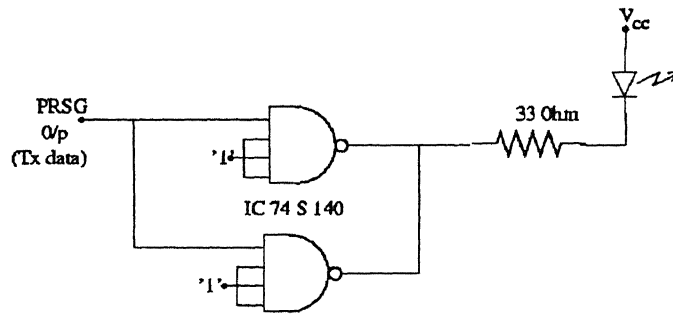


Fig 4.10a. LED Driver circuit with single LED.

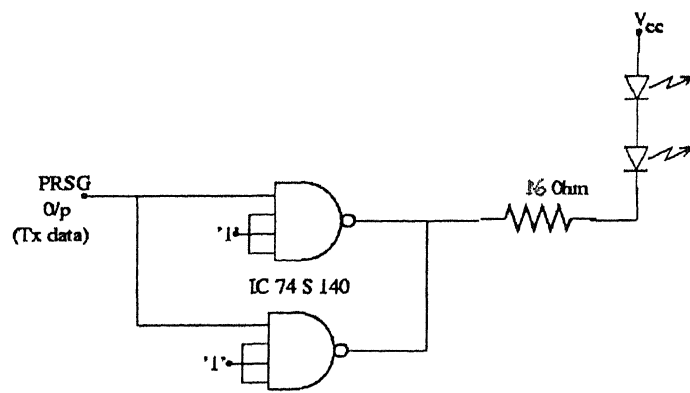


Fig 4.10b. LED Driver circuit with cascade of 2 LEDs.

4.4 RECEIVER CIRCUIT

The receiver circuit used in the setup is shown in Fig.4.11. Various stages of the receiver are detector, trans-impedance amplifier, peak detector circuit , summer, and comparator. Each stage of the receiver is discussed in the sections below.

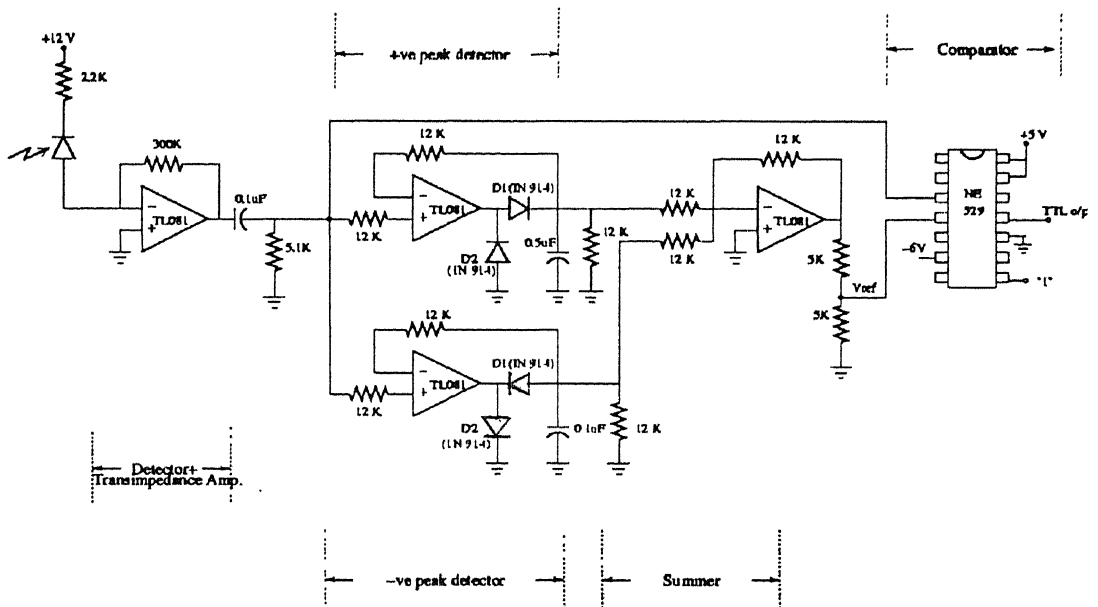


Fig 4.11 Receiver circuit .

4.4.1 Detector and the Pre-amplifier Circuit

The detector used in our receiver circuit was RCA C-30808. A reverse bias voltage of 12V was applied and the detector was connected to a transimpedance type preamplifier.

circuit realized using TL-081 operational amplifier (opamp). The feedback resistor used was 300K which was a good tradeoff between bandwidth of the preamplifier and the signal output. The important parameters of the C-30808 detector are given below.

Dark current	= 20nA
Radius of active area	= 1.26mm
Maximum bias voltage	= 15V
Responsivity at 820 nm	= 0.6 A/W
Capacitance (typical)	= 5 pF

The detector had smaller active area radius and was well suited for applications up to data rates of several Mbits/sec.

To improve the accuracy of the measurements, ambient light was kept to a bare minimum. Under no signal conditions it was found that the preamplifier output voltage was between 2 to 3mv. This is well within the specified dark current limit (20nA) of the detector. In the presence of IR signals the preamplifier output was close to 1V which was sufficient for the subsequent sections of the receiver.

4.4.2 Peak Detector Circuits

In contrast to point-to-point links one of the greatest challenges in the design of a receiver circuit for diffused links is the requirement of large dynamic range. The receiver circuit should correctly recover when the transmitter is very close to the receiver as well as when it is located far from the transmitter. Under such conditions simple threshold comparator will give rise to errors. To solve this problem peak detector circuits were designed and implemented to detect both high and low peaks of the received signal. These peak detectors were implemented using TL-081 opamps.

The positive (high) peak detector as shown in Fig.4.11, measures the positive peak values of the received signal. During the positive half-cycle of v_{in} , the output of the operational amplifier drives D_1 on, charging capacitor C to the positive peak value V_p of the input voltage v_{in} . Thus, when D_1 is forward biased, the op-amp operates as a voltage follower. On the other hand, during the negative half-cycle of v_{in} diode D_1 is reverse biased, and voltage across C is retained. The only discharge path for C is through R_L since

the input bias current I_B is negligible. For proper operation of the circuit, charging time constant (CR_d) and discharging time constant (CR_L) must satisfy the following conditions:

$$C R_d \leq T/10 \quad (4.1)$$

where R_d = resistance of the forward biased diode, 100 ohms, typically.

T = time period of the input waveform and

$$C R_L \gg 10T \quad (4.2)$$

where R_L is very small so that equation(4.2) cannot be satisfied, use a buffer (voltage follower) between capacitor C and load resistor R_L . although TL081 type op-amp is used in the circuit of figure(1), a high- speed , precision- type op-amp such as the uA771, or uA714 may be desirable in critical applications. The resistor R is used to protect the op-amp against the excessive discharge currents, especially when the power supply is switched off. the resistor $R_{om} = R$ minimizes the offset problems caused by input currents. In addition, diode D_2 conducts during the negative half cycle of v_{in} and hence prevents the op-amp from going in to negative saturation. This in turn helps to reduce the recovery time of the op-amp. Similarly, the negative peaks of the input signal v_{in} can be detected simply by reversing diodes D_1 and D_2 as shown in Fig.4.11.

4.4.3 Summer using Op-amp:

The TL081 op-amp was used for summing the outputs of the positive and negative peak detectors. The out put of summer is given by,

$$V_o = -R(V_P/R - V_N/R) = - (V_P - V_N) \quad (4.3)$$

The summed output at pin 6 of the op-amp is applied to a potential divider, made up of two resistors of same value in series, to obtain half the summed output as the reference voltage for the comparator NE529.

4.4.4 Comparator Circuit using NE529

NE 529 is a high speed analog voltage comparator which uses schottky diode technology with the conventional linear process. This allows simultaneous fabrication of high speed TTL gates with a precision linear amplifier on a single monolithic chip. It has a propagation delay time of 10ns and provides complementary output gates. This IC also has

wide common mode and differential voltage ranges. The preamplifier output was applied to one of the comparator inputs with the other input set at half the signal amplitude.

4.5 RECEIVER CHARACTERISATION

The performance of the above receiver was evaluated. The major receiver parameters are sensitivity, maximum data rate capability and dynamic range. Measured results for these are given below.

4.5.1 Receiver Sensitivity :

Receiver sensitivity is defined as the minimum received signal power required to obtain a certain Bit error rate or SNR (signal-to-noise ratio) performance. The sensitivity of the above receiver was found to be -35 dBm (300nW approx.) at a data rate of 200 kbits/sec.

4.5.2 Dynamic Range

The dynamic range gives the allowed variation in the input optical power. This is an important parameter for diffused links. The dynamic range of our receiver was found to be 30 dB at 200Kbits/sec. The large dynamic range is because of the adaptive threshold scheme used in our receiver.

4.5.3 Maximum Data Rate

The maximum data rate capability of the circuit was about 800 Kbits/sec. However the sensitivity and dynamic range were quite inferior at this data rate. Hence in all our experimental work data rate was fixed at 200kbits/sec.

4.6 SYSTEM MEASUREMENTS AND PERFORMANCE

The data transmission capability of the IR link was tested using different sources and the transimpedance receiver. The major measurements were

- (i) Variation of optical power as a function of the axial distance (longitudinal separation) from the source
- (ii) Variation of optical power as a function of the lateral distance for a particular axial distance.

4.6.1 Longitudinal Separation Measurement

This measurement was carried out by fixing the source at a place and moving the power meter along the axis of the source in a straight line. The power received was found to decrease rather faster as the axial distance was increased. The measured results for the four types of sources, viz. round LED, cut LED, 3-LED array and 5-LED array are shown in Fig.4.12 – Fig.4.15. From the results it is seen that the power variation along the axis is slower for the array LEDs as compared to the single sources. The variation is the slowest for the case with 5 LEDs.

4.6.2 Lateral Separation Measurement

Optical power measurements were also carried out for the LED sources for various lateral separation distances keeping a certain longitudinal distance between the source and the detector. These results are given in Fig.4.16 – Fig.4.19 for round LED, cut LED, 3-LED array and 5-LED array, respectively. The longitudinal distance in each case is also indicated.

4.7 COMPARISON OF THEORETICAL AND MEASURED RESULTS:

The experimental and theoretical results were compared for the longitudinal separation cases using the theoretical results of Models 1 and 2.

Fig.4.20 – Fig.4.23 compares the measured and theoretical results assuming the source to have intensity patterns of the form $I(\theta) = I_0 \cos^n \theta$, for longitudinal separation cases. In each case the best value of n that matches the corresponding far-field pattern is used. The agreement is not good except for the single round LED case.

Fig.4.24 – Fig.4.27 gives similar results for the theoretical Model-2 assuming uniform power distribution. In each case the measured results are compared with theoretical graphs for θ values of 24° , 60° , 84° . The single cut type LED results appear to be agreeing reasonably well. Other measured results does not agree well with theory.

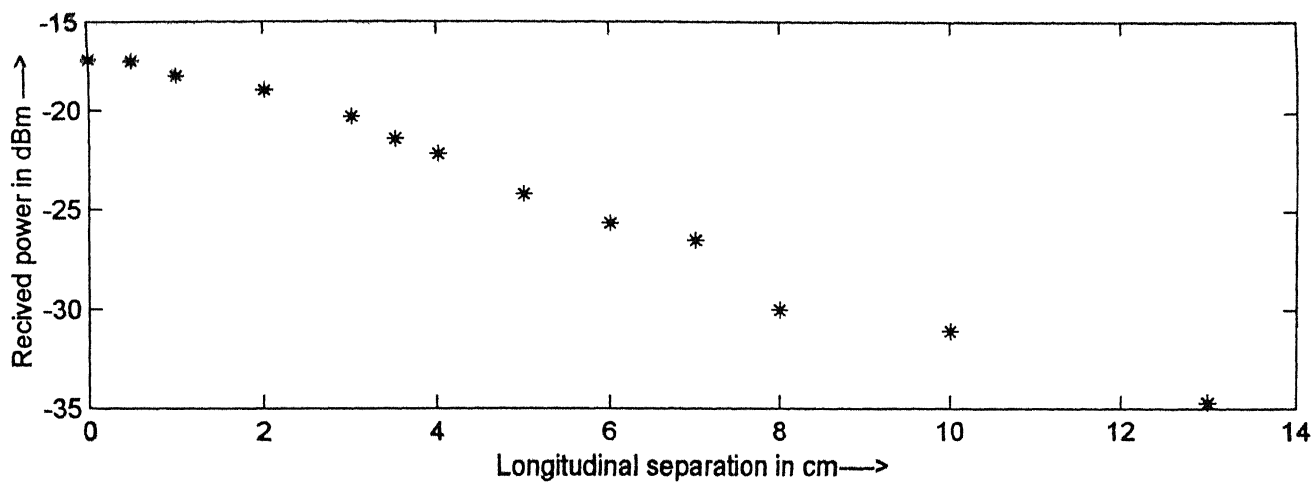


Fig4.12 Longitudinal offset of round type of IR LED

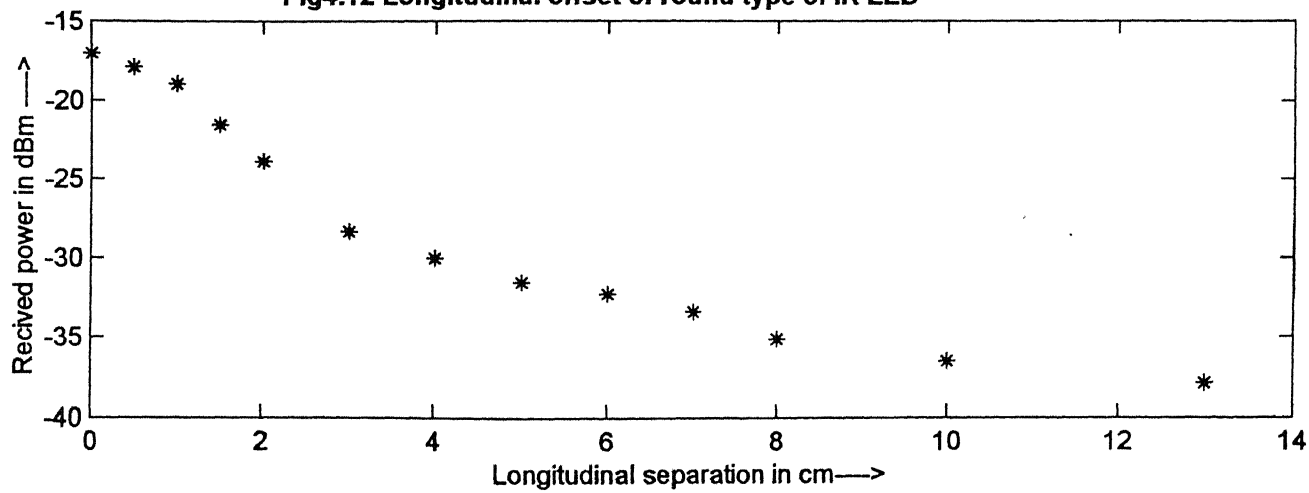


Fig4.13 Longitudinal offset of cut type of IR LED

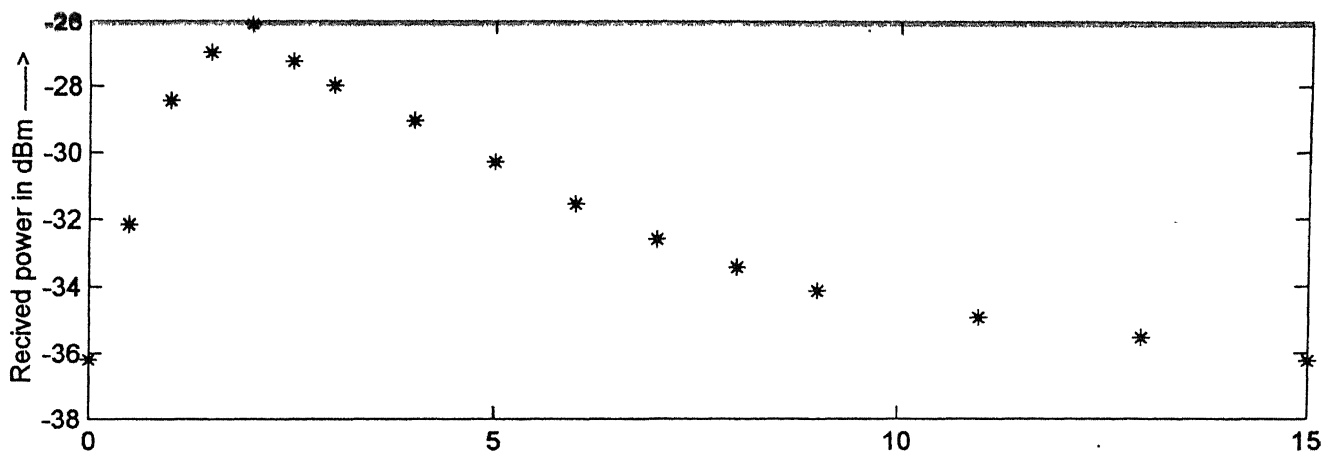


Fig 4.14. Longitudinal offset of array(3no.) of IR LED

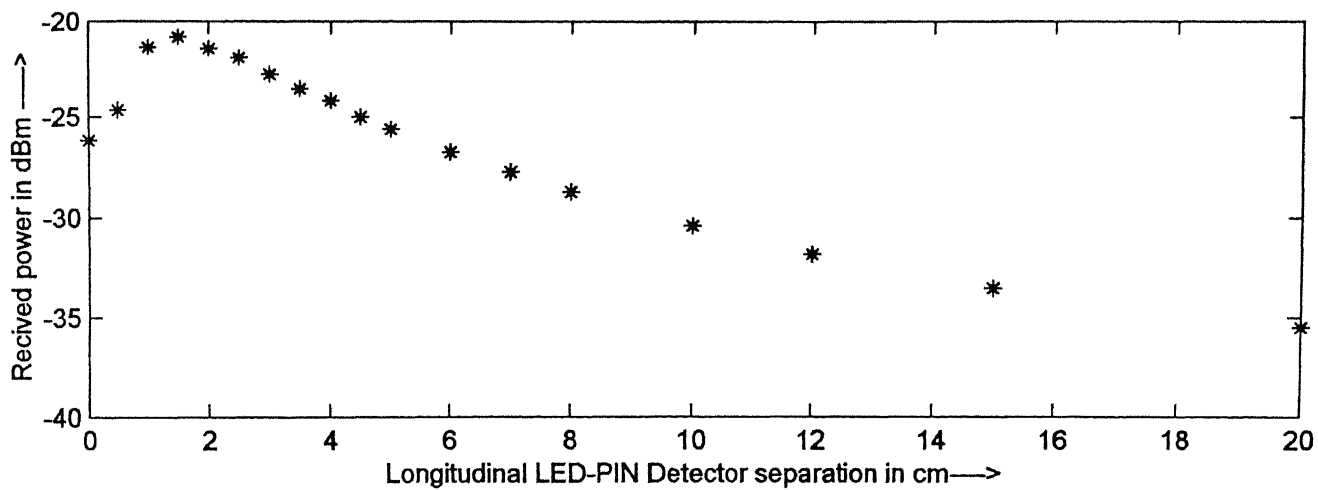


Fig 4.15. Longitudinal offset of array(5no.) of IR LED

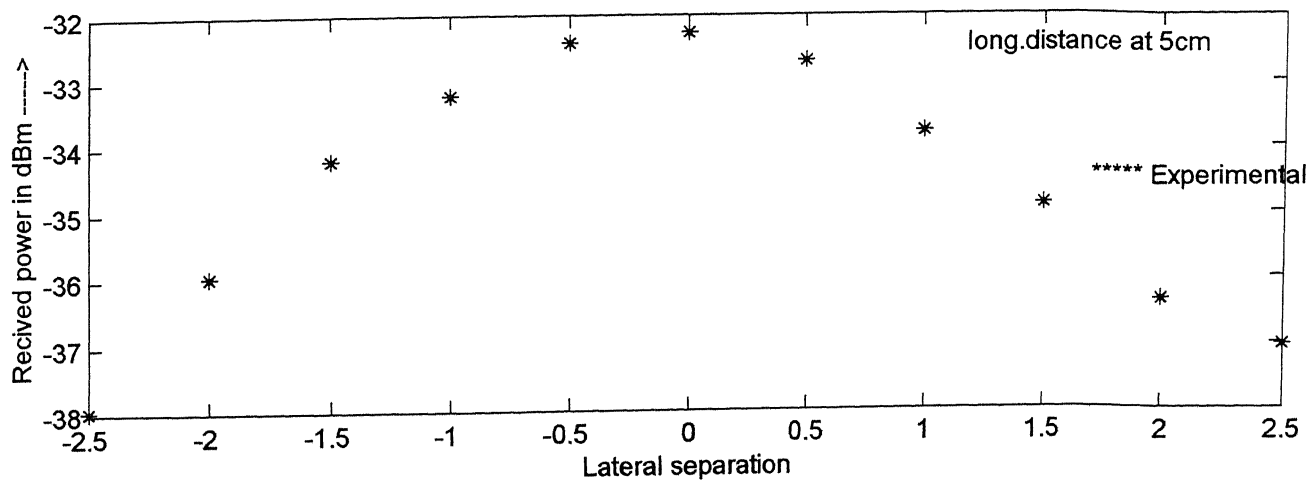
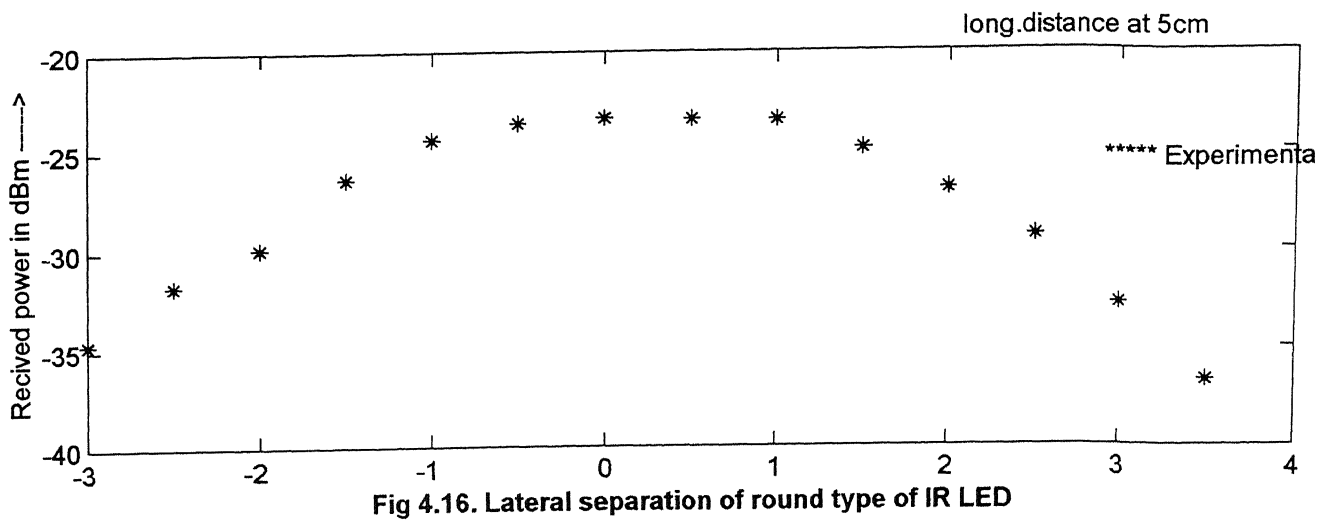
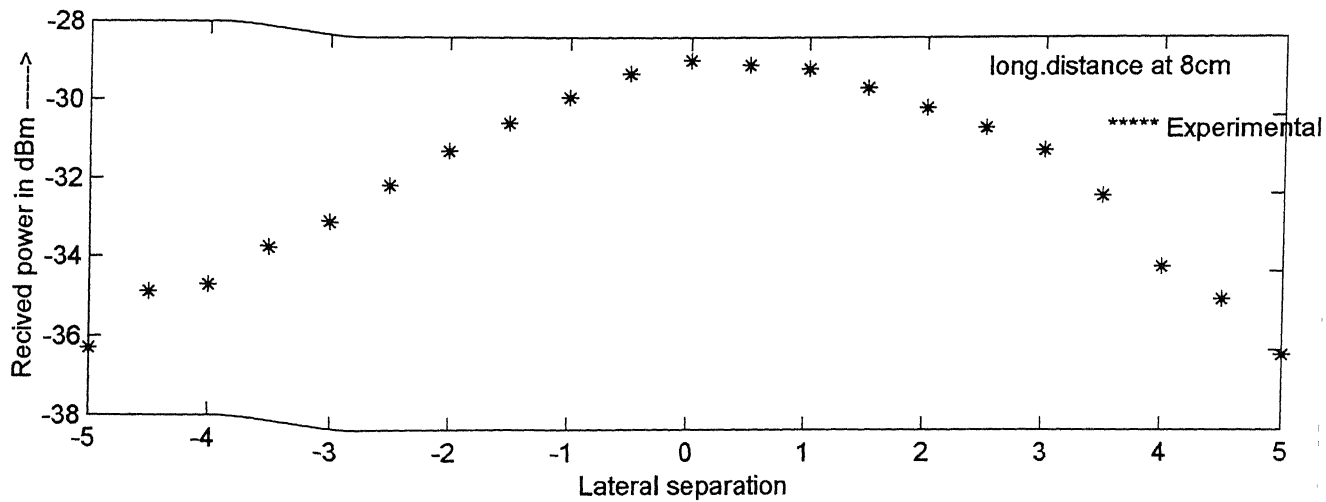
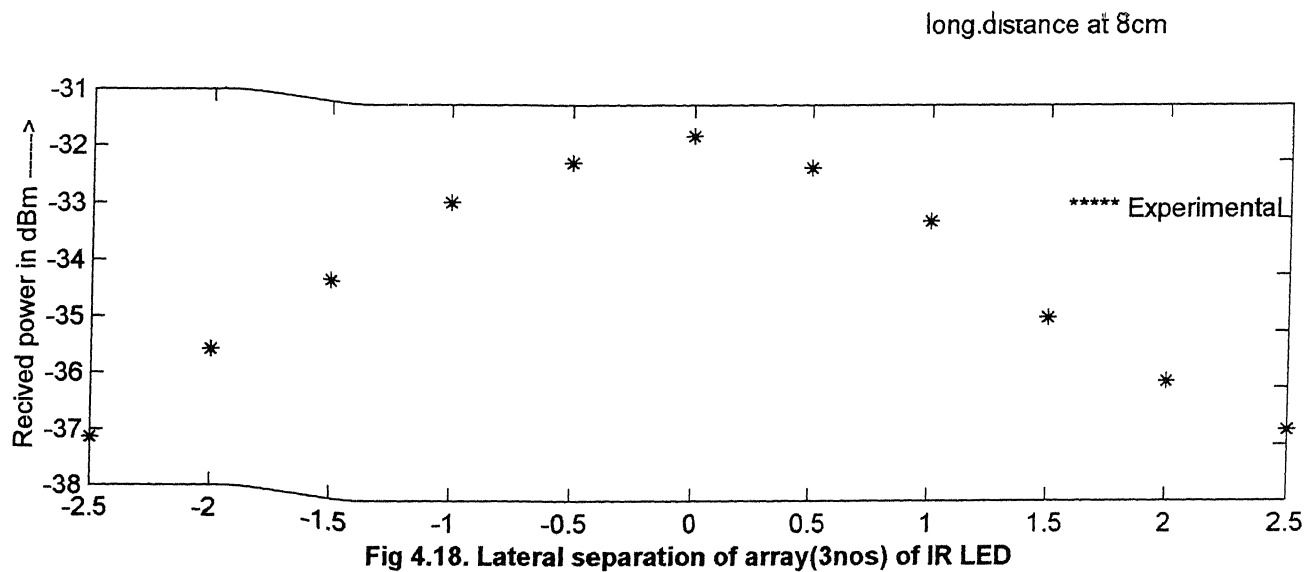
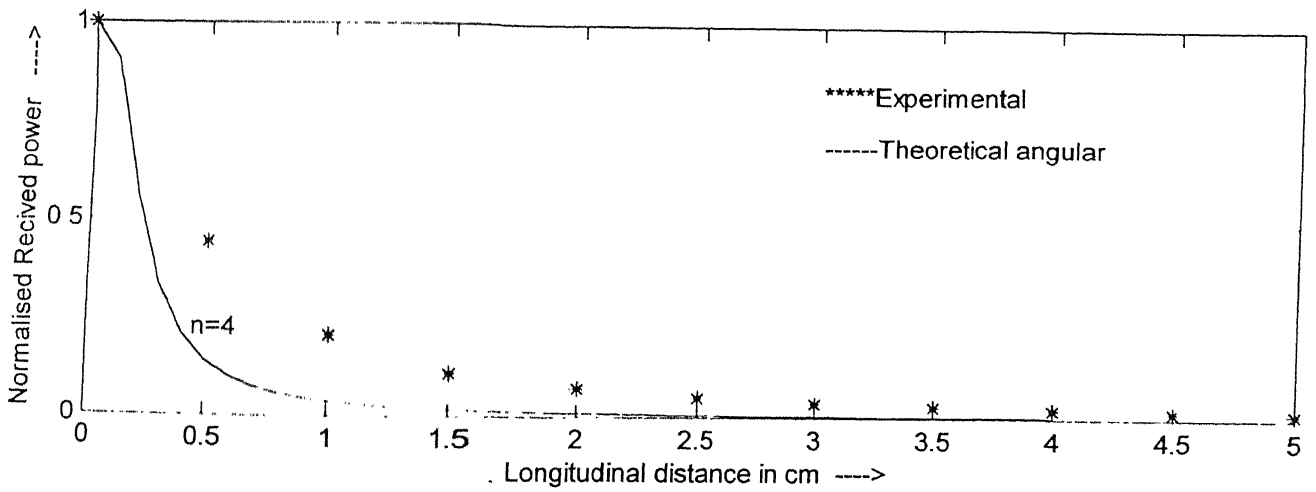
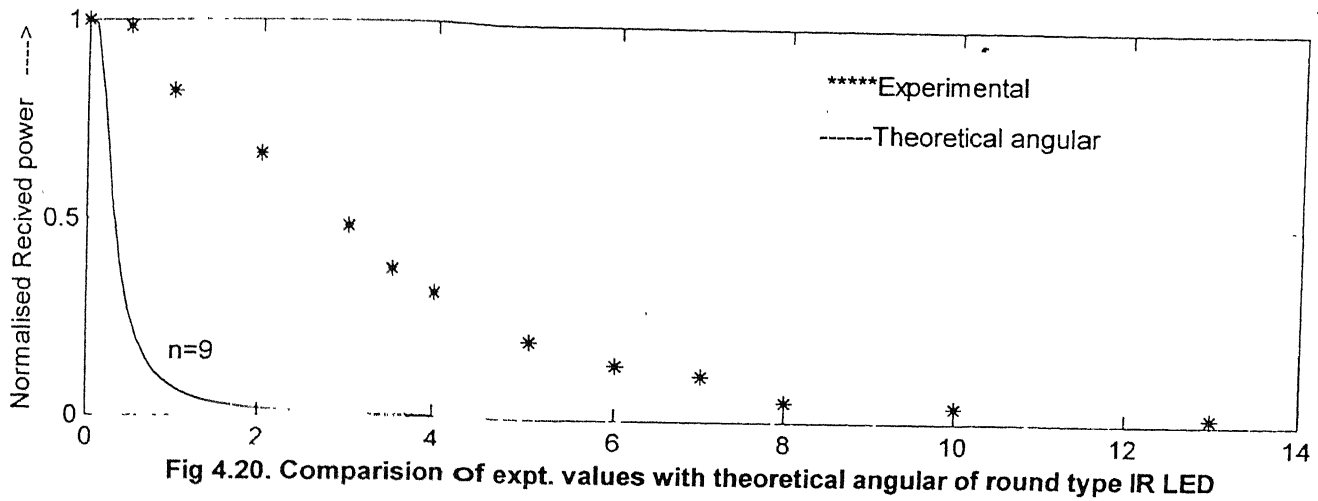


Fig 4.17. Lateral separation of cut type of IR LED





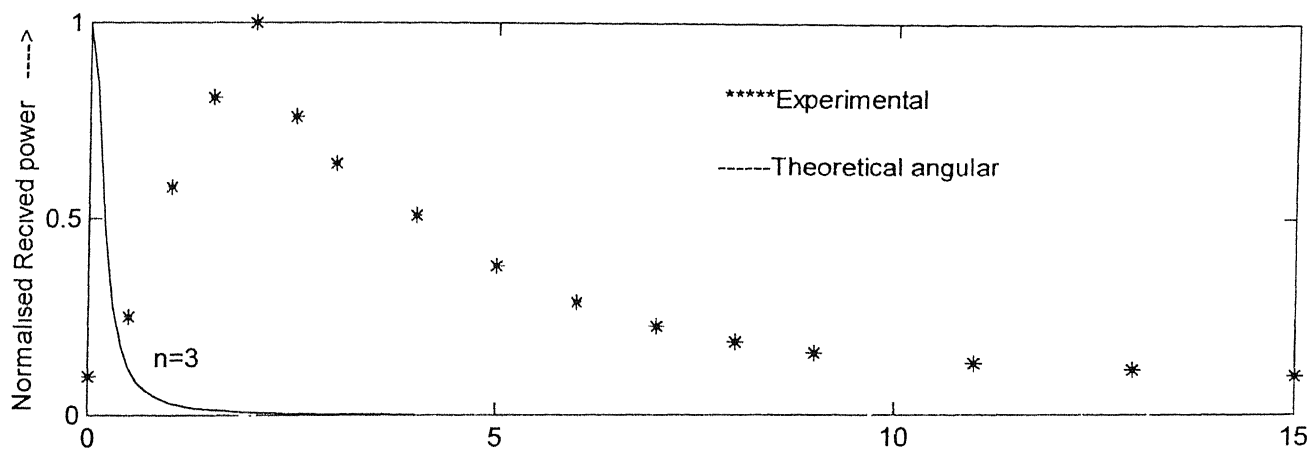


Fig 4.22. Comparison of expt. values with theoretical angular of array(3nos) IR LED

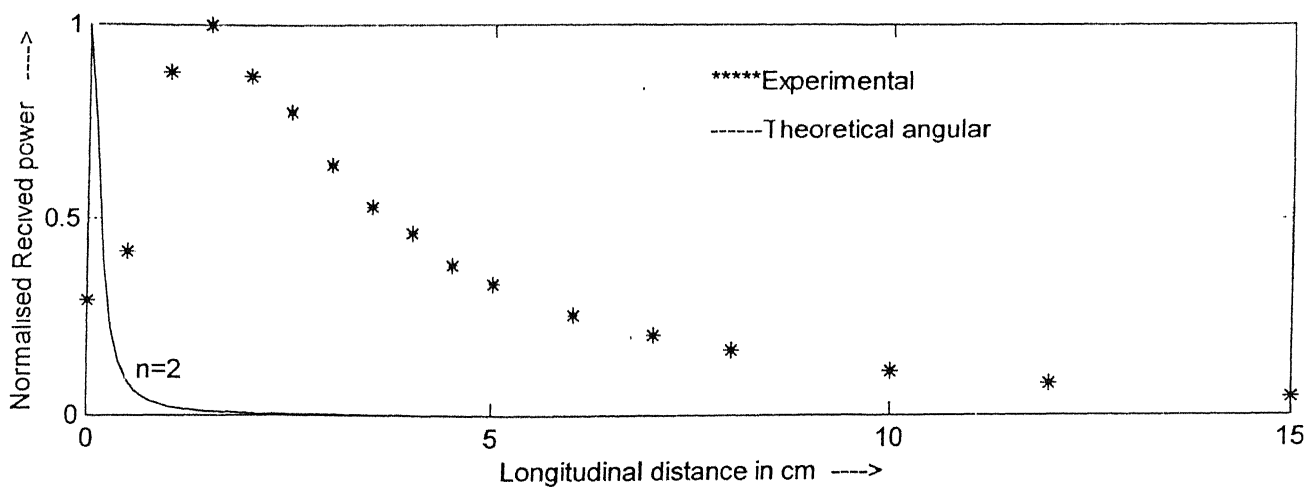
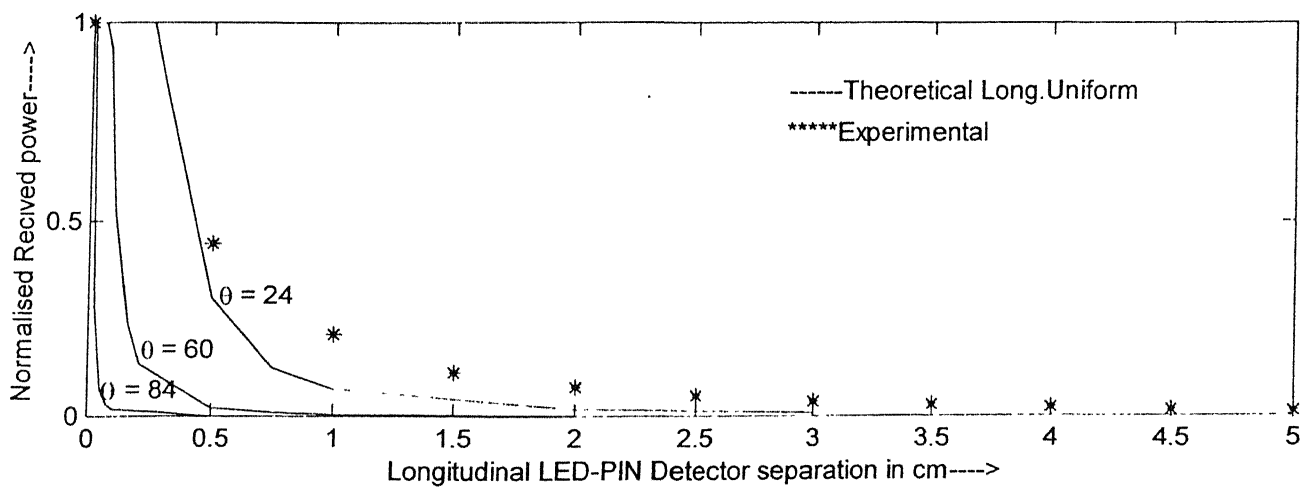
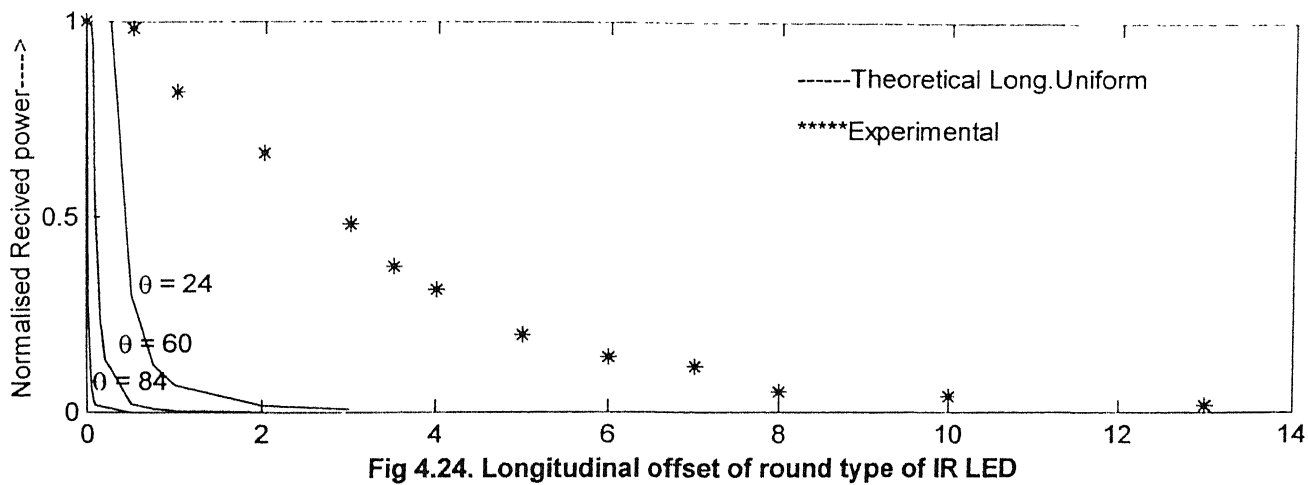
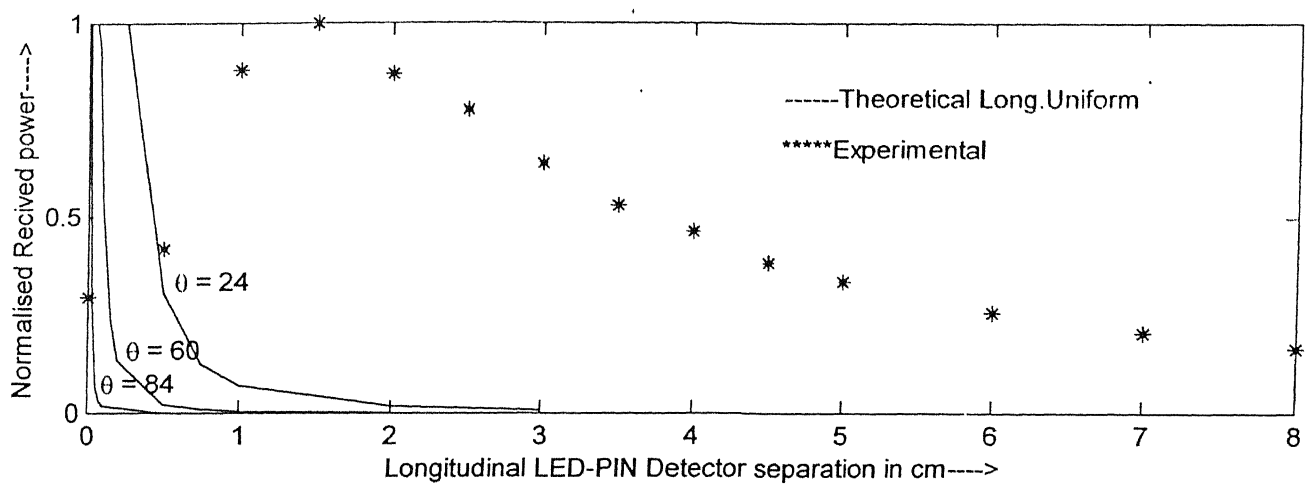
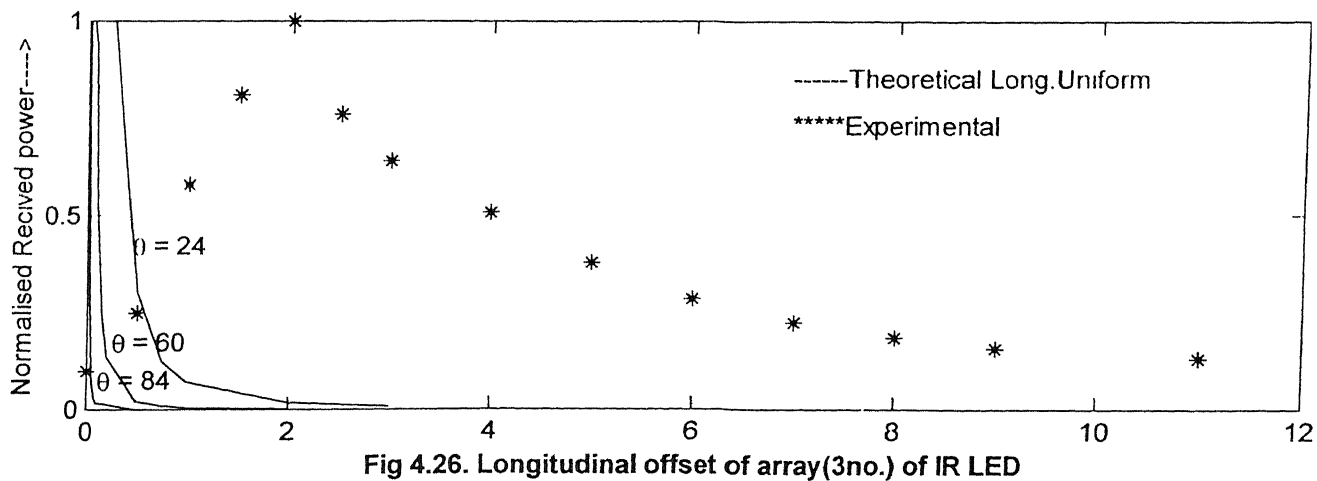


Fig 4.23. Comparison of expt. values with theoretical angular of array(5nos) IR LED





RESULTS, CONCLUSIONS AND SUGGESTIONS FOR FUTURE WORK

RESULTS AND CONCLUSIONS

The present work was aimed at studying diffused indoor optical wireless systems. A detailed review of indoor optical wireless systems was given in Chapter 2.

Design of an indoor IR was taken up using LED sources and PIN photodetector. As part of the theoretical study some models used in the power coupling area were attempted for predicting optical powers along the longitudinal direction.

Far-field patterns of four types of LED sources were measured and best fits were attempted using Gaussian and $I(\theta) = I_0 \cos^n \theta$ models. The fits were found to be good.

Parameters of the IR link such as sensitivity, dynamic range and maximum data rate and range were also measured. The sensitivity of the op-amp based receiver was found to be about -35 dbm at a data rate of 200 kbits/sec. The dynamic range was found to be 30dB. The maximum range for single LED sources was about 8cm at 100mA of LED current, while that of the 3-LED array and 5-LED array were 15cm and 20cm, respectively.

Variation of optical power along the axes of the four types of LED sources were measured and compared with two models, viz. the $I(\theta) = I_0 \cos^n \theta$ model and the uniform power distribution model. The agreement between theory and experiment was in general not good.

Power measurements were also carried out for various lateral separation cases for a given longitudinal separation. These results were also plotted for all the four sources.

In conclusion diffused Optical wireless systems were found to be well suited for indoor applications. In order to improve range high power LED array sources must be chosen and must be arranged in such a fashion so as to make them radiate in all directions. Our study showed that a proper hemispherical layout with several LEDs will improve the range considerably.

In our work we did not use optical filters to prevent ambient light. The use of optical filters will greatly improve the sensitivity of the optical receiver.

SUGGESTIONS FOR FUTURE WORK

The major strength of the present work is that a lot of experimental work was done to understand the system constraints and bottlenecks of indoor IR links. The present work lacks good theoretical models in analysing and predicting optical powers away from the source. Some work should be done in this direction.

REFERENCES

- [1] F.R.Gfeller and U.H.Bapst, "Wireless In -House Data Communication via Diffused Infrared Radiation," *Proceedings of the IEEE*, vol.67, No. 11, pp. 1474-1486, Nov 1979.
- [2] K.Pahalvan, "Wireless Communication for Office Information Networks," *IEEE Communication Magazine*, vol.23, june 1985, pp. 19-27
- [3] A.M.Street , " Indoor Optical Wireless Systems -Overview," *Optical & Quantum Electronics*, No.29, 1997, pp. 349-378.
- [4] T.S.Chu and M.J .Gans , " High Speed Infrared Local wireless Communication ," *IEEE Communication Magazine* , vol.25, No.8, pp.4-10, Aug 1987.
- [5] Jose Fernandes, PA Watson and J.Neves, " Wireless LANs: Physical properties of Infrared Systems vs Mmw Systems," *IEEE Communication Magazine* , Aug 1994.
- [6] J.Kahn and j.Barry, "Wireless Infrared Communications," *Proceedings of the IEEE*, vol.85, No.2 , Feb. 1997, pp. 265-298.
- [7] J.R.Berry et al . " High Speed Non-directive Optical Communication for wireless Network," *IEEE Network Magazine*, vol.5, No.6, Nov.1991, pp.44-54.
- [8] J.R.Berry, J.M Kahn, W.J.Krause, E.A .Lee and D.G.Messerschmitt,"Simulation of Multipath Impulse Response for Wireless Optical Channels," *IEEE Journal on selected Areas in Communication*, vol.11, No.3, pp.367-379, April 1993.
- [9] J.R.Berry et al, " Non-directed Infrared links for High Capacity Wireless LANs," *IEEE Personal Communication*, second quarter 1994, pp.12-25.
- [10] G.W. Marsh and J.M.Kahn, " Channel Reuse Strategies for Indoor Infrared Wireless Communications," *IEEE Transactions on Communication*, vol.45, No.10, Oct 1997, pp.1280-1290.
- [11] H.Hashemi, G.Yung, M.Kavehrad, R. Behbahani and P.A.Galko, " Indoor Propagation Measurements at Infrared Frequencies For Wireless LAN Applications," *IEEE Transactions on Vehicular Technology*, vol.43, pp.562-576, August 1994.
- [12] Kaveh Pahlvan, "Wireless Data Communications" *Proceedings of the IEEE*, vol.82, No.9, sept 1994.

- [13] J.B.Carruthers and J.M.Kahn, " Modeling of Non-directed Wireless Infrared Channels," *IEEE Transactions on Communication Engg.*, vol .45, No.10, Oct 1997, pp. 1260-1268.
- [14] R.Narsimhan, M.D. Audeh and J.M.Kahn, " Effect of Electronic Ballast Fluorescent Lighting on wireless Infrared Links," *IEE Proceedings on Optoelectronics.*, vol.143, No.6, Dec. 1996, pp.347-354.
- [15] K.Pahlavan, T.Probert, and M.Chase, " Trends in Local Wireless Networks," *IEEE Communication Magazine*, Mar 1995, pp.88-95.
- [16] AF Gfeller , Walter Hirt , " A Robust Wireless Infrared System with Channel Reciprocity," *IEEE Communication Magazine*, Dec 1998.
- [17] David J.T.Heatley, et. al, " Optical Wireless: The Story So Far, " *IEEE Communication Magazine*, Dec 1998.
- [18] F.Chow and JM Kahn , " Effect Of non-reciprocity on Infrared Wireless LANs," *IEEE Communication Magazine*, Dec. 1998.
- [19] J.M.H.Elmirghani, " New PPM-CDMA hybrid for Indoor diffuse IR Channels," *Electronics Letters*, vol.30, no.20, pp.1646-1647, 29/9/94.
- [20] David P.Johnson, D.J.Cowar, " Free Space IRLAN(FIRLAN)," *Optical Engg.*, vol. 32, No. 9, pp. 2114-2117, sept'1993.
- [21] Lee Goldberg, "IR Data Transmission:The missing Link," *Electronic Design*, pp . 47-64, 17/4/95.
- [22] Humayoon Saam, " Coping with convergevce:The future of wireless system design," *Electronic Design*, pp.67-70, 6/1/97.
- [23] J.B.Carruthers and J.M.Kahn, " Angle Diversity for Non-direted Wireless Infrared Commn.,"*IEEE Transactions on Communication*, june 2000, pp. 960-978.
- [24] JM Kahn, Roy You at el, " Imaging Diversity Receivers for high speed Infrared Wireless Commn.," *IEEE Communication Magazine*, Dec1998.
- [25] P.Djahani and JM Kahn , "Analysis of Infrared Wireless Links employing Multibeam Transmitters and Imaging Diversity Receivers," *IEEE Transactions on Communication*, july 1999.
- [26] J.M.Kahn, " Compound Parabolic Concentrators for Narrow band Wireless IR Receiver," *Optical Engg.*, vol,34, No.5, pp. 1385 – 1395 , may 1995.

- [27] M.D Audeh, J.M.Kahn and J.R .Berry, "Performance of PPM on measured Non-directed Indoor Infrared Channels," *IEEE Transactions on Communication*, vol.44, pp. 654-659, June 1996.
- [28] H.Park and J.R.Barry, "Performance of multiple PPM on multipath channels," *IEE Proceedings on Optoelectronics*, vol.143, No.6, Dec.1996, pp.360-364.
- [29] G.W.Marsh and J.M.Kahn, " Performance Evaluation of experimental 50-Mb/s Diffused Wireless Link using On-Off keying with Decision –Feedback Equalization ," *IEEE Transactions on Communication* , vol.44, No.11, pp.1496-1504, Nov 1996.
- [30] M.D.Audeh, J.M.Kahn and J.R.Berry, " Decision –Feedback Equalization of PPM on measured Non-directed Indoor Infrared Channels," *IEEE Transactions on Communication*, vol.47, pp . 500-503, April 1999.
- [31] C.R.Lomba, R.T.Valdas, " Experimental Characterization and Modeling of the Reflection of IR signals on Indoor surfaces," *IEE Proceedins on Optoelectronics*, vol.145, No.3, pp. 191-197, June 1998.
- [32] B.P.Crow et al, " IEEE 802.11 wireless LAN draft standad," *IEEE Communication Magazine*, pp.116-126, Sept 1997.
- [33] Brian Ingham, Richard Helm, "IR role in Wireless communication expands with IrDA," *Electronic Design*, pp.62-68, 21/7/1997.
- [34] Glenn R. Elion, Herbert A. Elion, "*Fiber Optics in Communication Systems*", Copyright ,Marcel Dekker,Inc.,1978.
- [35] Prakash Veer , "*Studies on Light Emitting Diode to Multimode Fiber Coupling*", MTech Thesis report, April 1996.
- [36] M.K.Barnoski(Ed.) , "*Fundamentals of Optical Fiber Communications*" , Academic Press Inc., New York, 1976.
- [37] Vandana Tak , "*Improvement of Coupling efficiency between LED and MM Fiber using Grin rod Lens*", M.Tech Thesis report , May 1998.
- [38]. Sandeep Kumar , "*Studies on Multimode Fiber to PIN Photodetector Coupling*" , M.Tech. Thesis report , March, 1995.
- [39] Completion Report , " *System Design and studies of Fiber Optics Digital Communication Systems*" , A Project Sponsored by DRDO.

133748



133748

Date Slip

The book is to be returned on
the date last stamped.

This image shows a blank sheet of white paper with horizontal blue ruling lines. A single vertical red margin line runs down the left side of the page, creating a narrow left margin. The paper appears to be from a notebook or a standard writing template.